ANNUAL REPORT 1985

NASA Technical Memorandum 87179

RESEARCH & TECHNOLOGY

LEWIS RESEARCH CENTER

NASA
National Aeronautics and Space Administration

Contents

Introduction

This report summarizes the NASA Lewis Research Center's research and technology accomplishments for fiscal year 1985. The report is organized into five major sections covering aeronautics, aerospace technology, spaceflight systems, space station systems, and computational technology support. This organization of the report roughly parallels the organization of the Center into directorates. Where appropriate, subheadings are used to identify special topics under the major headings.

The results of all research and technology work performed during the fiscal year are contained in Lewis-published technical reports and presentations prepared either by Lewis scientists and engineers or by contractor personnel. In addition, significant results are presented by university faculty or graduate students in technical sessions and in journals of the technical societies. For the reader who desires more information about a particular subject, the Lewis contact will provide that information or references.

In 1985, five Lewis products were selected by Research & Development Magazine for IR-100 awards. All are described and identified in this report. In addition, the Lewis Distinguished Paper for 1984-85, which was selected by the Chief Scientist and a research advisory board, is included and so identified.

For general information about this report, contact Robert W. Graham at (216) 433-5828, or FTS 297-5828.

Aeronautics

Instruments and Controls

Advanced Sensor Failure Detection for Aircraft Engine Controls

The objective of the Advanced Detection, Isolation, and Accommodation (ADIA) program is to demonstrate satisfactory engine control system operation after a system sensor has failed. The ADIA program is based on the principle of analytical redundancy. A dynamic model of the engine (an analytical function) as well as the sensed engine variables is used to generate redundant estimates of the sensed variables. The redundant estimates are then compared with the sensor outputs to detect failures.

The ADIA algorithm was developed by using advanced decision and control theories. The development consisted of defining the problem, specifying five competing ADIA strategies, screening competing strategies to select the best, and evaluating the winning strategy on an engine test-bed system. The test-bed system was a non-real-time simulation of the F100 turbofan engine and the F100 multivariable control system. The algorithm detects, isolates, and accommodates both hard and soft failures over a full operating range of the engine. Hard sensor failures are large, instantaneous failures that have a strong effect on system operation. Therefore they are easily detected. Soft failures, on the other hand, are small and can occur slowly (such as a drift). By their nature soft failures are more difficult to detect. As a result the logic to detect soft failures is much more complicated than that for hard failures.

The algorithm was successfully implemented by using standard Intel 8086/8087-based microprocessor hardware. The computing power requirements were met by using three identical processors in a parallel-processing environment. The programming of this algorithm on the microprocessor system was significantly simplified by using Fortran and floating-point arithmetic.

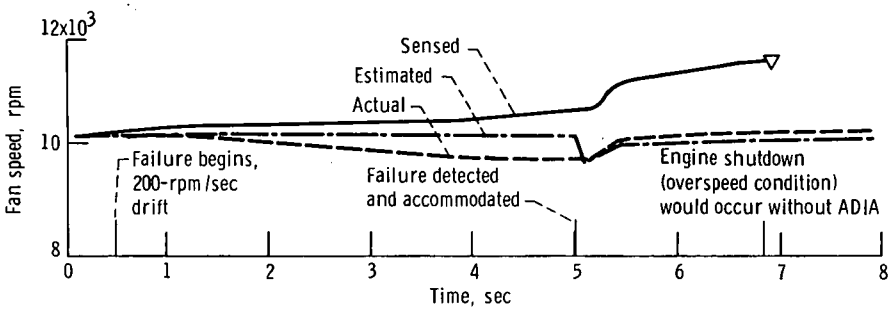

Fan speed sensor failure—hybrid simulation results

Real-time algorithm performance and implementation integrity were evaluated by using a hybrid computer simulation of the F100 engine. The evaluation demonstrated the value of soft sensor failure detection. It is planned to demonstrate the algorithm on a full-scale F100 engine in the altitude test facility. This program builds on the highly successful F100 Multivariable Control program, which was tested in this facility in 1979. □

Systems for Whole-Field Flow Measurement

Significant progress has been made in extending the capabilities of optical flow visualization techniques to provide quantitative flow data, needed in wind tunnel and gas turbine research, by using an easily automated readout method. For the first time an electronic heterodyne technique was applied to a moire deflectometry system to improve both the accuracy and the sensitivity of moire fringe pattern measurement. Concurrently an electronic heterodyne holographic interferometry system was developed and evaluated for the quantitative analysis of double-pulse holograms. The two extremely sensitive systems were then successfully compared in laboratory tests by using a flow simulator. Both techniques are compatible with computer-controlled readout and data processing.

The moire system has a wide range of sensitivities and can be used as a real-time or photographic system; the more sensitive holographic system does not require high-quality optical access to the flow field. □

High-Power Arc Lamp for High-Heat-Flux Experiments

In the late 1960's there arose a need for a high-power arc lamp to produce solar flux on large experimental bodies in NASA Lewis' space propulsion chamber at the Plum Brook Station. The need to produce up to two solar constants on a 100-ft^2 area led to the design of a 400-kW arc lamp that was 20 times the size of then-available lamps. A key portion of the technology developed for this lamp was the electrode design to handle the high heat loads.

Lewis is now engaged in designing heat flux sensors for turbopump research for the space shuttle main engine (SSME). Heat fluxes experienced in the SSME can be 50 times those in aircraft engines. No existing facility can calibrate such sensors. A calibrator now being designed is based on a commercial arc lamp developed and manufactured by Vortek Industries Ltd. in Canada. This lamp, with power to 300 kW, was developed by Vortek from Lewis electrode technology. They then added significantly to the arc technology by developing a unique vortex flow of water and gas within the arc tube to both contain the arc and keep the tube clean.

Thus a commercial product needed for today's shuttle engine technology arose from Lewis technology developed for solar simulation in the 1960's. □

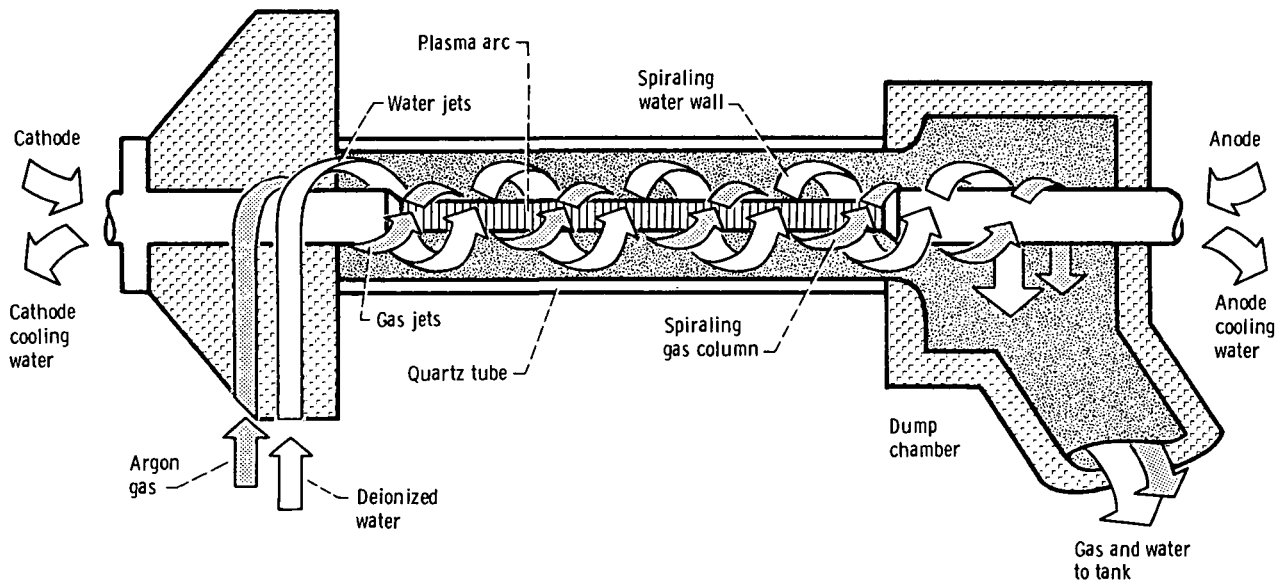

Vortek arc lamp

Internal Fluid Mechanics

Modeling the Internal Combustion Engine

Despite the apparent simplicity of the internal combustion engine, the complexity of interacting physical and chemical processes has defied complete understanding. Modeling the engine has been difficult because of the following factors:

(1) The system is open and operates at relatively high temperatures and pressures. It retains a memory of the preceding cycle because the cylinder is not completely evacuated at the end of each cycle and because the end of one cycle provides the initial conditions for the following cycle.

(2) The operation has a repetition rate ranging from 25 to 250 msec.

(3) Some complex hydrocarbon combustion chemistry is taking place, and the time scale for some of the chemical reactions is comparable to the cycle repetition rate.

(4) The system's movable boundaries and complex geometry complicate the fluid mechanics and heat transfer.

(5) The engine operation is not strictly repeatable because the engine undergoes apparently random cycle-to-cycle variations.

The net result of these factors is a system that exhibits strong temporal and spatial gradients during a cycle and relatively large fluctuations from one cycle to the next.

A mathematical model of the internal combustion engine has been constructed and implemented as a computer program suitable for use on a large digital computer system. The model and associated computer program are described comprehensively in NASA RP-1094. The report briefly reviews past experimental and modeling efforts and justifies the chosen modeling alternatives from the standpoints of experimental information and computational practicalities. It gives a detailed description of the mathematical models, the numerics, and the working fluid's physical properties. The report concludes with a series of example calculations to illustrate the capabilities of a hierarchy of five models that vary from a simple thermodynamic model to a complex model requiring full combustion kinetics, transport properties, and poppet-valve flow characteristics.

The computer program based on the models reproduces the major features of the internal combustion engine and is computationally both flexible and economical. It can perform multicycle calculations, permits cycle-to-cycle variations in parameters, and makes provisions for restarting calculations. It allows revision of the working fluid's physical properties and changes in operating conditions, engine parameters, and modeling functions. The flexibility of the computer program permits calculations to be carried out at a level of complexity consistent with the level of knowledge about a particular engine. □

Turbulent Boundary-Layer Separation and Reattachment

Lewis is making a continuing effort to calculate the flow through turbomachinery blade rows. An accurate computation, of course, depends on the ability to model all of the flow phenomena encountered within the passage. One phenomenon that has been difficult to model is a blade surface turbulent boundary layer that separates from the surface, forms a separation bubble, and subsequently reattaches to the blade surface.

Lewis has contracted with the United Technologies Research Center to simulate this flow in large size in their low-speed, two-dimensional, boundary-layer wind tunnel. Separation bubbles approximately 50 cm long and 15 cm high have been formed on a flat-plate surface. Visualization studies and very detailed measurements of the flow within and around the separation bubble have been made by using laser anemometry. These results can serve as a basis for formulating new flow models with which to calculate this flow phenomenon or for verifying that analytical codes can accurately compute this flow. □

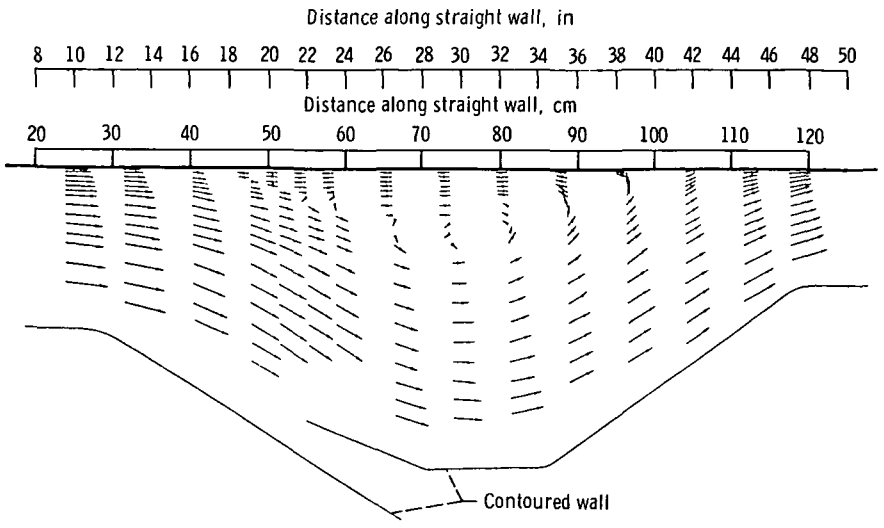

Laser Doppler velocimeter measurements on wind tunnel centerline

Heat Transfer in Heat Exchanger Passages

Many heat exchanger applications require that the heat transfer per unit area be maximized with the least pressure drop. A multipass heat transfer scheme in which the flow changes direction several times is sometimes used. In a cooling application this approach yields an efficient use of the coolant by substantially raising its temperature. Roughness elements are also used to give a high level of heat transfer.

An experimental program was undertaken to determine the heat transfer characteristics of a single multipass loop. The heat transfer after a bend was found to be very similar to the heat transfer after an abrupt entrance. High entrance-region heat transfer was observed along a significant length of the duct. This entrance effect was evident even when the base level of heat transfer was increased by using roughness elements on the heat transfer surfaces.

Although roughness elements (ribs) augment the heat transfer over a smooth-walled duct, they also increase the pressure drop in the duct. An experimental program was conducted to determine if ribs set at an angle would result in better performance than ribs normal to the flow. Ribs at an oblique angle were found to significantly lower the pressure drop in the duct while maintaining the same heat transfer. □

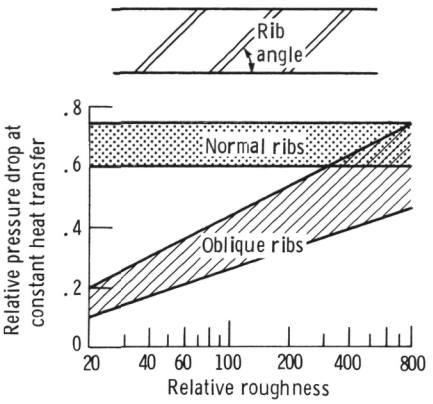

Pressure drop in heat exchanger passages as function of roughness

Propulsion Systems

Ceramic Matrix Combustor Liner

Higher gas turbine engine cycle efficiency and lower fuel consumption can be realized by increasing cycle pressure ratio and turbine inlet temperature or implementing advanced cycles such as the regenerative/recuperative cycles. Conventional combustors operating at these conditions require more cooling air than is readily available. Thus there has been much recent interest in engine application of high-temperature ceramic and composite materials, which require little or no coolant and minimize use of strategic materials. Previous research has shown that ceramics are prone to stress failures induced by thermal shock. If, however, a ceramic is sprayed on a plyable substrate, a major improvement in thermal cyclic fatigue results. In the ceramic matrix liner concept, ceramic is bonded to a flexible metallic layer,

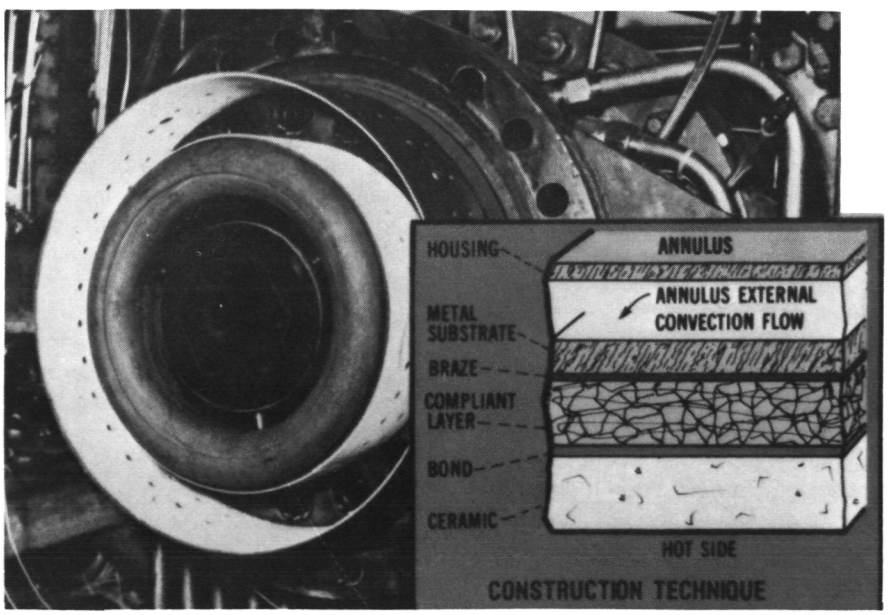

Ceramic matrix combustor liner

which in turn is brazed to a support structure.

Performance experiments were conducted on a full-scale NASA-designed annular combustor with ceramic matrix liner walls. The liners, constructed of nonstrategic materials, incorporated only back-side convective cooling. Injection of film or transpiration coolant into the combustor, mandatory for current-technology designs, was not required. Good short-term durability was demonstrated to outlet temperatures of 2630 °F, at least 300 deg F hotter than current practice. The measured liner temperatures were less than 1600 °F, which is well within design limits. Thus it appears that this liner approach is an ideal candidate for implementing efficient engine cycles. □

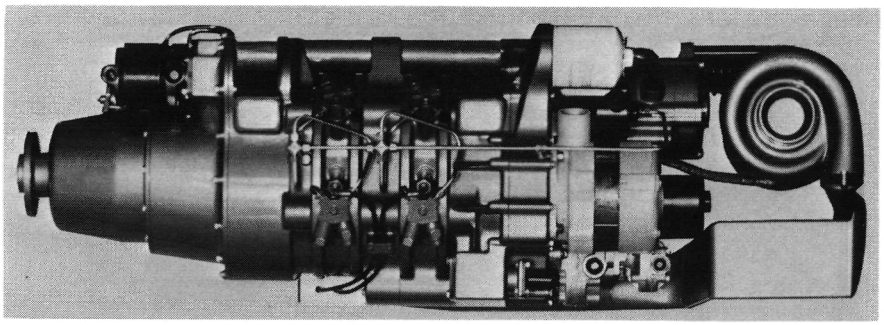

State-of-the-art rotary engine

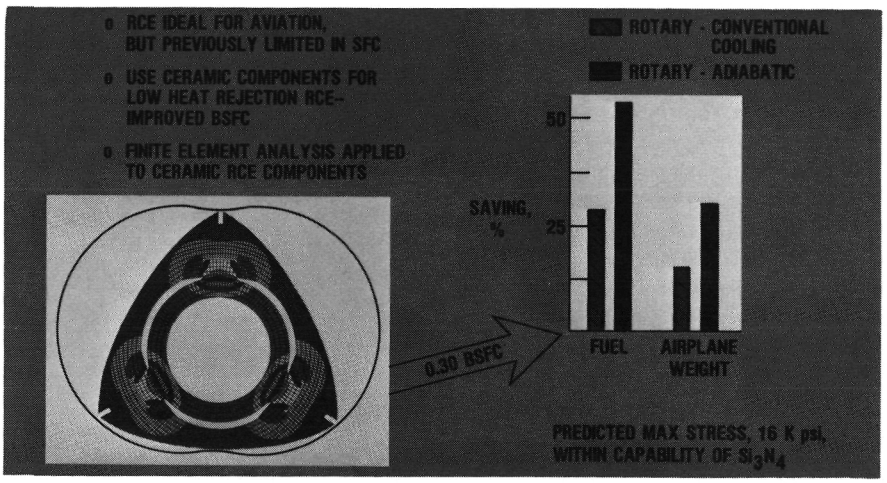

Ceramic components

Ceramic Rotary Engines

Previous studies and experiments have shown the rotary combustion engine (RCE) to be a viable and highly attractive candidate for light aircraft. Through inherent characteristics such as multifuel capability, smoothness, and low-cost producibility, this unique engine combines desirable features that otherwise exist separately in small turbines and reciprocating engines. As a result of NASA-sponsored efforts, significant new manufacturing commitments for the production of aircraft RCE's have been made by Avco, John Deere and Co., and Teledyne since 1984. A jet-fuel-burning RCE is expected to enter service in 1990, the first new light-aircraft powerplant in over 30 years.

During 1985, a study by Adiabatics, Inc., identified further major growth potential through the use of advanced ceramic materials. In brief, the few and comparatively simple parts of the RCE are ideally suited to ceramic coatings or monolithic ceramic construction. The resulting high-temperature, nearly adiabatic engine should provide more than twice the power from the same size package as well as brake specific fuel consumption to match that of the adiabatic diesel.

During 1985, finite-element studies of a ceramic rotor (the most critical component) were conducted. Maximum stress levels (16 000 psi) are within the present capabilities of silicon nitride and are less than half of those predicted for comparable ceramic components (pistons and turbines) in diesel and turbine engines. This suggests the early application of ceramic rotors to RCE's. Further analyses, including those of other ceramic structural components and an overall thermal and stress model, have recently been started. □

Airfoil Performance in Icing

Aircraft performance degradation (increased drag and decreased lift) due to ice accretions on unprotected surfaces can be severe. However, the need for greater aircraft efficiency dictates that ice protection be provided only for the most critical components. Thus performance degradation on unprotected surfaces is currently being determined in icing wind tunnel tests and flight tests.

NASA Lewis, as part of the aircraft icing program, is developing an analytical capability for predicting aircraft performance in natural icing conditions. Emphasis is currently being placed on the prediction of airfoil performance degradation due to leading-edge ice accretions by using both thin-layer Navier-Stokes and interactive boundary-layer codes. A complementary experimental program is being conducted to map in detail the flow fields about airfoils with leading-edge ice accretions in order to provide a comprehensive code-validating data base.

Thin-layer Navier-Stokes predictions of airfoil lift and drag characteristics were compared with measurements for an NACA 0012 airfoil with an artificial leading-edge ice accretion. The analytical predictions that were made by assuming turbulent boundary-layer growth from the stagnation point agreed closely with the experimental data. However, predicted and measured velocity profiles at two points within the separation-reattachment zone downstream of the ice accretion differed. The differences were attributed to either grid characteristics, ice shape definition, or turbulence modeling. All three areas are being investigated. Only recently has an interactive boundary-layer approach been applied to the problem. This approach is viewed as being complementary to the Navier-Stokes approach in that the execution times are approximately one order of magnitude less.

A thoroughly validated analytical approach to aircraft icing offers an attractive and cost-effective alternative to the more conventional approaches featuring icing wind tunnel and artificial/natural icing flight testing. □

Ceramic Component Technology for Low-Heat-Rejection Diesel Engines

Lewis is pursuing advanced technologies in support of the Department of Energy's efforts to develop the uncooled, low-heat-rejection (LHR) diesel engine as part of its petroleum conservation program. The LHR diesel engine shows promise for reducing fuel consumption by recovering normally wasted exhaust heat energy through turbocompounding or other bottoming systems. To improve the efficiency of such systems, insulating materials are used to control heat losses and to elevate the exhaust temperature. It is generally agreed that ceramic materials are the key to effective designs for this new environment, but monolithic ceramic insulators have experienced continuing structural problems. An alternative is the use of ceramic thermal barrier coatings applied to conventional metal components.

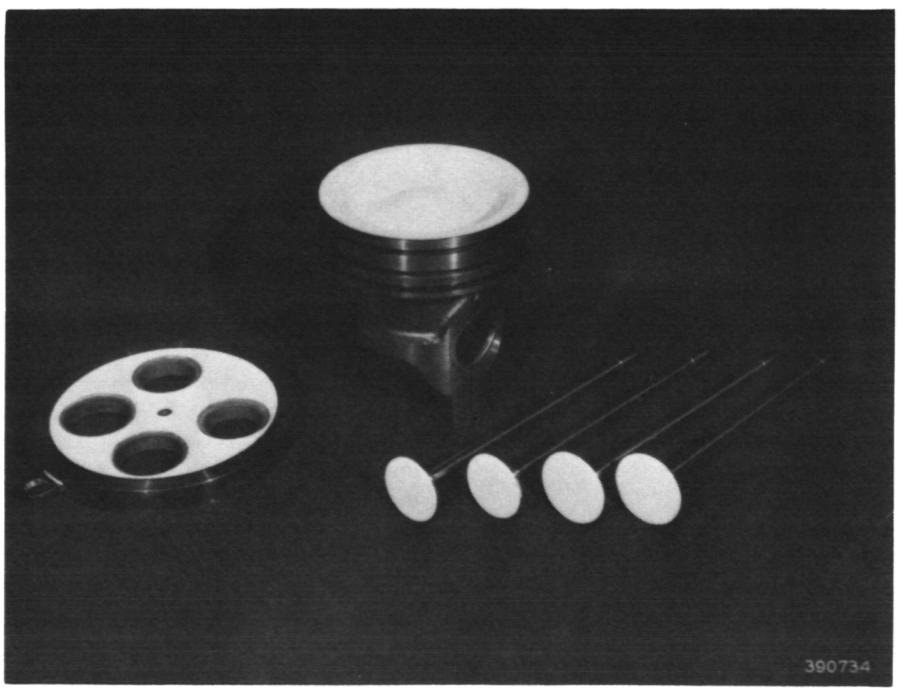

Ceramic-coated components ready for installation in LHR diesel engine

Lewis has contracted with the Detroit Diesel Allison Division of the General Motors Corporation to develop thick ceramic coatings with thermal effectivenesses competitive with those of monolithic ceramics. In this program, zirconia coatings were successfully applied to such engine components as the firedeck, valves, and piston cap of a single-cylinder diesel engine. The 0.100-inch-thick coating (0.060-in.-thick ceramic coating applied over a 0.040-inch-thick strain insulator pad) has a thermal conduction rate equivalent to that of a 0.300-inch-thick monolithic zirconia component. It has survived a 24-hour engine test with minimal distress. Plans are being formulated for more severe engine tests of this promising thermal barrier coating.

The elevated operating temperatures of the LHR diesel engine also pose severe tribological problems, particularly at the interface of the piston ring and cylinder liner. No known liquid lubricants can survive at surface temperatures of 1200 °F, such as are expected in the top ring reversal region. Lewis has a contract with the Southwest Research Institute (SRI) to develop or improve monolithic ceramic materials suitable for unlubricated operation as piston rings and cylinder liners. The four highest rated materials from the program are K–162B (a nickel-molybdenum-based TiC cermet), TiC, Si_3N_4, and SiC. The wear rates for these materials under

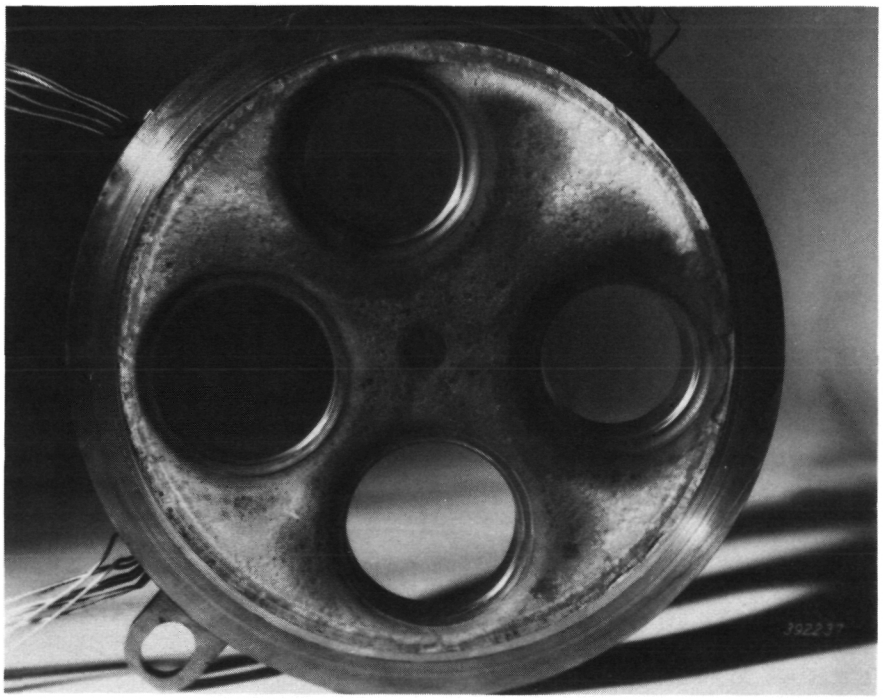

Firedeck of LHR diesel engine after test

nonlubricated conditions at approximately 1500 °F were reasonably good, particularly for the K–162B and TiC. The friction coefficients need improvement although the K–162B is competitive with high-temperature, solid-lubricated materials. SRI is investigating surface treatment effects such as ion implantation in an effort to improve the friction and wear characteristics of monolithic ceramics. □

Ceramic Component Technology for Gas Turbine Engines

As part of the Department of Energy's Automotive Technology Development program, Lewis is working to develop a technology base applicable to an automotive gas turbine engine. Gas turbine engines offer the potential of significant fuel savings over conventional internal combustion engines and have emission levels that meet or surpass current or proposed Federal standards. Technology development contracts are in place with the Allison Gas Turbine Operations of General Motors Corporation and with the Garrett Turbine Engine Company. Development of ceramic components able to withstand 2500 °F is critical to the overall success of the program.

During 1985, significant progress was made in ceramic component technology development. Ceramic static structures have been undergoing extensive analysis, design modification, and engine environmental testing at temperatures to 2100 °F. Continued efforts in fabrication development have produced ceramic rotors with excellent dimensional control and surface finish. These rotors have been successfully spin tested at room temperature to 137 000 rpm (150 percent of rated speed) and are currently in the initial phases of engine environmental testing. All activities are progressing toward testing a complete set of ceramic components in a test-bed engine at temperatures to 2500 °F by the end of 1986. □

Successful Demonstration of Convertible Engine

Lewis has recently demonstrated the dual-mode and conversion capability of the convertible engine. This revolutionary engine concept could enable rotorcraft to maneuver like helicopters but attain the cruising speeds of fast air transports by using helicopter rotor blades as fixed wings. The tests are part of a joint program by the Defense Advanced Research Projects Agency (DARPA) and NASA.

The engine is "convertible" in the sense that it can operate as a turbofan engine by disengaging the rotor, as a turboshaft engine driving the rotor in the helicopter mode, or in both modes simultaneously. A sophisticated digital electronic system would be used to control the vehicle throughout all modes of operation.

In operation the projected craft would take off vertically through the use of a lifting rotor. When it achieved desired altitude and forward speed, the engine would convert from powering the rotor to a forward thrust or turbofan mode. The transmission would be disengaged and the rotor blades locked into a fixed position, their airfoil configuration imparting conventional lift to the plane for forward, level flight. Conversion from shaft power to forward thrust would take about 15 to 20 sec.

During 1985, the steady-state performance characteristics of the convertible engine as a turbofan, as a turboshaft, and in both modes simultaneously have been evaluated. In December 1984, the first transient operations simultating the conversion from rotary-wing to fixed-wing flight and the reverse were successfully accomplished. Conversion times were 18 sec. The engine responded as predicted during the conversions.

These tests represent the first successful operation of a 5000-hp-class convertible engine in both fan and shaft modes and the first dual-mode operation for the variable inlet guidevane concept. A new breed of high-speed rotorcraft using convertible engines would provide jet transport vehicle characteristics typical of airline operations, but with vertical takeoff and landing features. □

Convertible-engine rotorcraft

Structural Integrity of Advanced Propfans

New technology is being developed for application to highly loaded, multiblade propellers (propfans). These propfans use 15 to 30 percent less fuel than advanced turbofan engines (50 to 60 percent less than today's turbofan fleet) and achieve speeds to Mach 0.85.

Encouraging wind tunnel test results are helping establish confidence in propfans as a viable future alternative to turbofan engines. Under the NASA-sponsored Large-Scale Advanced Propfan (LAP) program with Hamilton Standard, a 2-ft-diameter aeroelastic model of the large-scale (9-ft-diam) propfan was successfully run without classical flutter in a Lewis supersonic wind tunnel. Flutter-free operation of the propfan was attained at flight speeds to Mach 0.9 and rotational speeds to 9000 rpm. (The propfan was designed for Mach 0.8 and 8622 rpm.) Also, the propfan was structurally cleared for safe operation at angle of attack over a range of flight speeds. The successful results of this test program add confidence that the large-scale propfan will be free of any instabilities when tested in the NASA Propfan Test Assessment (PTA) flight program. □

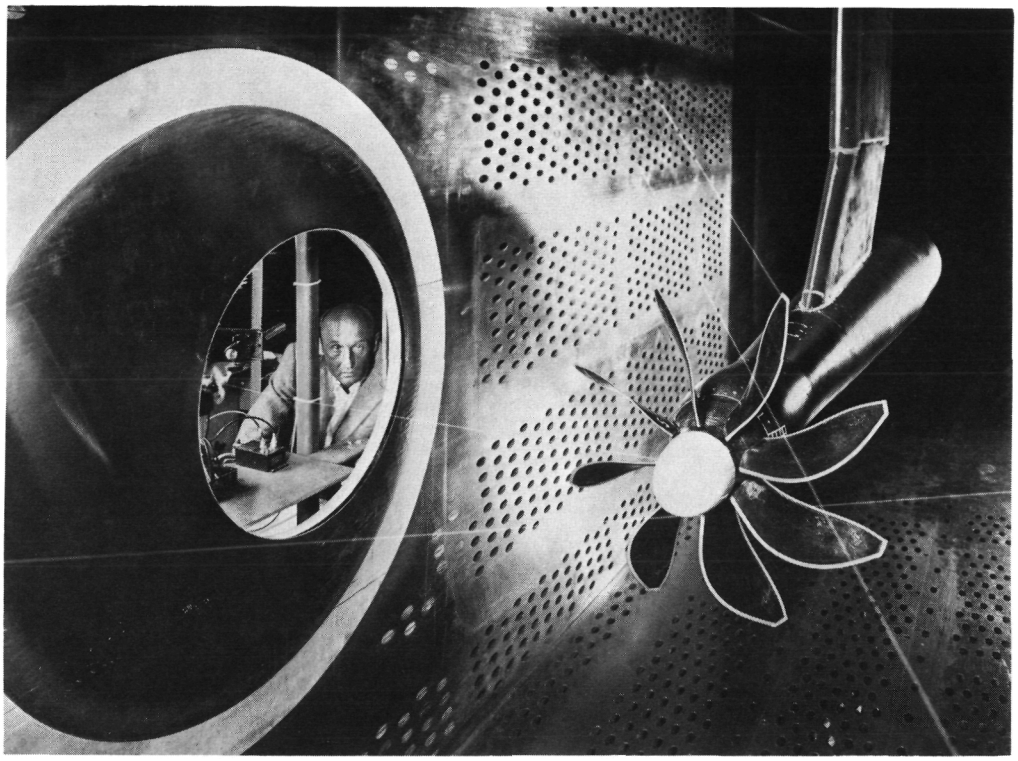

LAP model in wind tunnel, showing laser beam measurement of blade deflections

Modeling of Propfan Inlets

One of the problems associated with a propfan propulsion system is in designing a compatible engine inlet that provides high pressure recovery and low flow distortion at the compressor face without adversely affecting blade stress. The design problem is most acute with single-rotation (SR) tractor designs, where both axial and swirl velocity gradients due to the propeller must be considered. The inlet and diffuser must diffuse the air from a transonic Mach number to about Mach 0.4 at the compressor face.

Inlet performance has been investigated in joint NASA/industry experimental model programs involving Lockheed-Georgia, Hamilton Standard, United Technologies Research Center, Boeing, and Pratt & Whitney. Tests were performed with single-scoop, twin-scoop, and annular inlets. The effect of a boundary-layer diverter and the importance of cowl shape were also investigated. Further testing evaluated the effect of inlet proximity on propfan blade stress. An inlet S-duct diffuser model test was also conducted as part of the NASA-sponsored Propfan Test Assessment (PTA) program.

The single-scoop inlet offered the best performance of the various configurations because of its lower internal-boundary-layer buildup. The external-boundary-layer diverter significantly reduced inlet throat distortion and increased pressure recovery. Inlet blockage effects on the propfan resulted in higher inlet throat pressure recovery than predicted from isolated testing. Inlet location also had a significant effect on the blade stress, but acceptable values were obtained by increasing the distance between the propfan and the inlet at the expense of some reduction in pressure recovery.

Testing of the PTA S-duct diffuser model resulted in better than predicted pressure recovery with low levels of flow distortion, even with simulated swirl effects introduced. A properly designed large-scale SR tractor propfan inlet installation should recover enough of the propfan supercharging benefit at the compressor face to use about 2 percent less fuel than a similar SR propfan in a pusher installation. □

Performance of Counterrotation Propeller Models

Counterrotation (CR) propellers are attractive because they have the potential for eliminating the swirl losses associated with uninstalled single-rotation (SR) propfans. The CR would be 8 percent more efficient than the SR at Mach 0.8, assuming complete swirl recovery for the CR and none for the SR. According to a Hamilton Standard study, the CR would burn 9 percent less fuel than the SR on an advanced-technology 100-passenger aircraft.

Hamilton-Standard is conducting wind tunnel tests of their 2-ft-diameter 5×5-blade CR propfan model in an 8-ft tunnel. Preliminary aerodynamic performance results indicate peak propulsion efficiencies of 88 percent at Mach 0.7 and 86 percent at Mach 0.8 for this Mach 0.72 design. The test matrix is being expanded to provide aeroperformance data over a range of Mach numbers, tip speeds, and blade angles. Blade vibratory stress levels of this model were well below stress limits, and there was no evidence of any high-speed flutter.

In addition to the 5×5 CR model evaluated by Hamilton Standard, General Electric has evaluated, as a part of a joint NASA/GE experimental model program, a series of CR propfan blade designs in the Boeing transonic wind tunnel. These tests were in support of the unducted-fan (UDF) engine design, which will be evaluated in proof-of-concept ground static tests starting in September 1985. In contrast to the Hamilton Standard model, which has the propeller blades positioned for a standard front-mounted tractor installation, the blades of models used in support of the gearless UDF engine design are located well back on the nacelle (pusher configuration) with a blade hub-to-tip radius ratio about twice as large as the Hamilton Standard design. CR propfan efficiencies at the Mach 0.72 design point were higher than predictions for two of the three blade designs tested. Best design-point performance (85 percent efficiency) was obtained with the high-tip-sweep, low-aspect-ratio blade design to be used in the UDF demonstrator test. All three blade configurations also exhibited acceptable aeromechanical behavior, with low blade stress levels and flutter-free operation. □

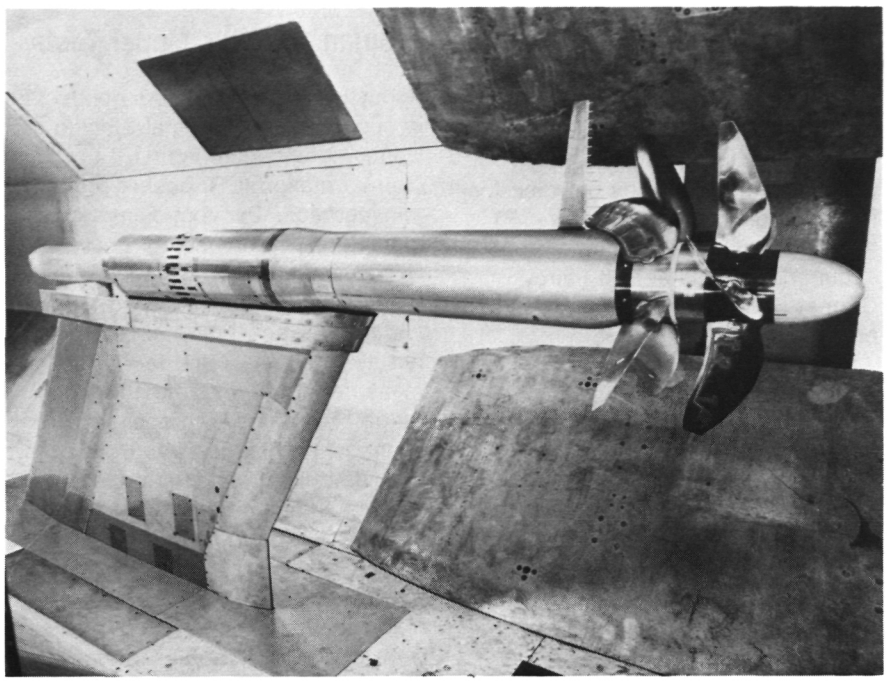

Hamilton Standard counterrotation propfan in wind tunnel

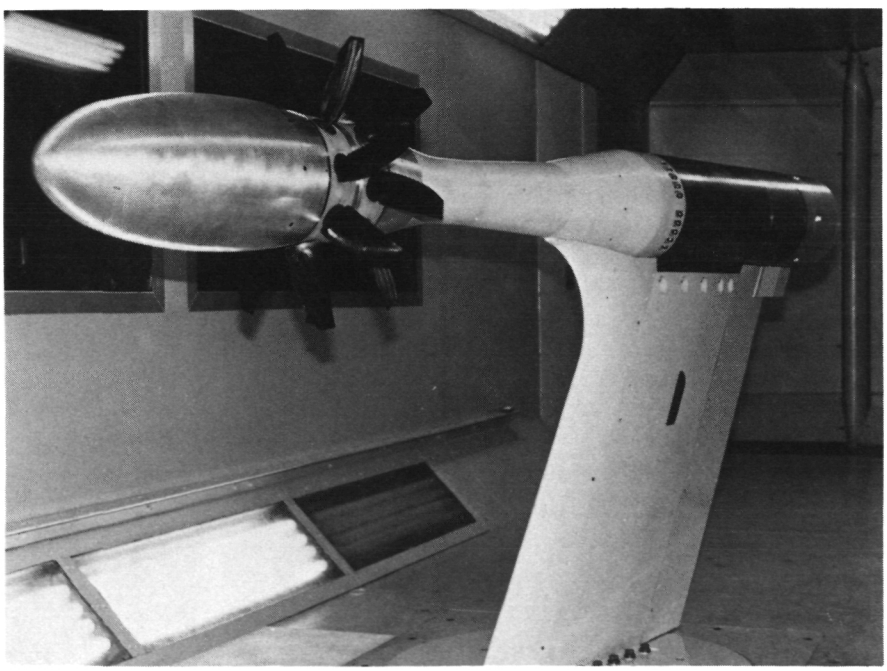

General Electric unducted-fan propfan in wind tunnel

Vibratory Response Test of Fairey-Gannet Counterrotation Propellers

To resolve questions about the adequacy of existing unsteady aerodynamic and structural analysis codes used to predict vibratory blade stresses resulting from the complicated interactions between the front and rear counterrotation (CR) blade rows, Hamilton Standard has acquired a 1950's design Fairey-Gannet British military aircraft with CR propellers.

Although these propeller blades are of a conventional thick, straight design, and the flight speeds were limited to about Mach 0.3, the good correlation obtained between measured stress data from the instrumented 4×4 CR propeller blades and prediction provides additional confidence in the analytical codes used in the design of new advanced CR blading. Additionally, CR operation was found to increase the 1P vibratory response of the rear propeller by about 25 percent over that obtained with SR operation; the effect of CR operation on the front propeller was negligible.

These test data will be useful in refining the analysis used to predict the aerodynamic interactions between the CR blade rows. These interactions affect both propeller acoustic and aerodynamic performance predictions. □

Propfan Acoustic Model Tests

Acoustic model tests were conducted in support of the General Electric Company unducted-fan (UDF) counterrotation (CR) pusher propeller configuration. Two-foot-diameter CR models respresentative of possible UDF blade configurations were tested in the Boeing transonic wind tunnel and the GE anechoic free-jet noise facility. Both near- and far-field noise measurements were taken over a range of tip speeds, propeller power loadings, and blade sweep, with simulated flight speeds typical of those used in community noise evaluations at FAR–36.

The results with these advanced, highly loaded, high-speed propellers were qualitatively similar to those obtained previously with more conventional CR designs. They had a broader directivity pattern than a previously tested comparable SR propeller and showed substantially more higher order spectral content than the SR as well. The community noise levels of these initial advanced CR configurations (after scaling the model data to full size) are projected to exceed the FAR–36 stage 3 limits at both the sideline and flyover (cutback) conditions.

To reduce the noise interaction between the two CR rotors, several model geometry variations were subsequently evaluated in the GE anechoic free-jet facility. Significant noise reductions were obtained with these design variants, and projections indicate that a CR propeller incorporating these features could meet the FAR–36 stage 3 requirements. □

Advanced Small-Engine Technology

NASA/Army studies have been conducted with turbine engine manufacturers to identify high-payoff technologies for small gas turbine propulsion systems in the year 2000. Gas turbine engines with shaft horsepower less than approximately 1500 hp do not perform as efficiently as larger turbine engines. NASA is developing a plan to augment the ongoing base R&T effort and to focus this research on small engines. This program is to provide the technology to identify revolutionary improvements in small engines such that their performance will approach that of large engines. A goal of 50 percent reduction in fuel burned, greater reliability and durability, and lower cost has been set for the program.

To provide technology roadmaps to permit achieving these goals, five study contracts were awarded to industry. These contracts were jointly funded by the Army and NASA. A wide range of military and civil applications were studied by the contractors to include helicopters, commuter and general aviation aircraft, and cruise missiles. The approach to achieving the program goals encompasses the application of advanced cycles, more efficient components, and high-temperature, uncooled ceramic materials. The contracts are now complete, and the results are being used to develop the technology plans to be pursued under the Advanced Small Engine Technology (ASET) program. □

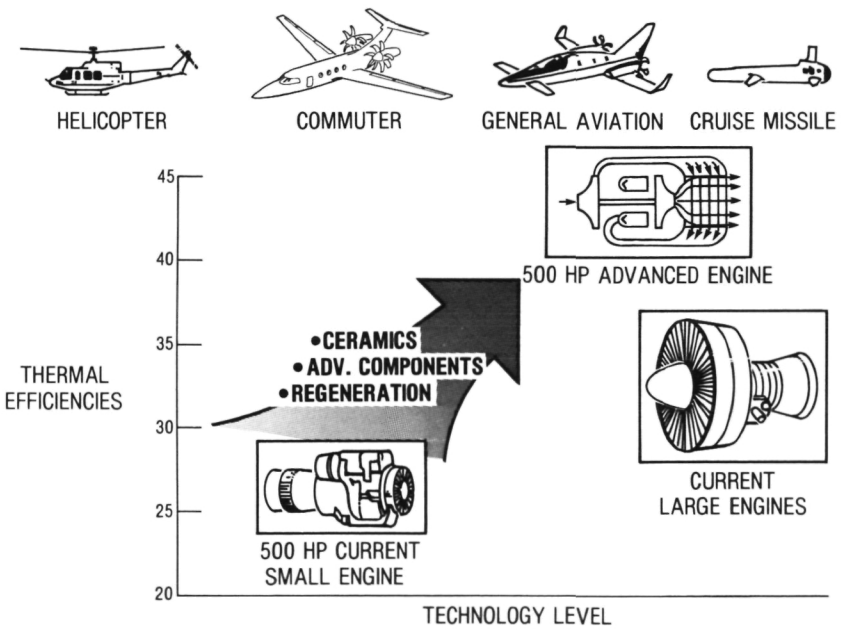

Small-engine technology

Regenerative Engine Cycles

Small turbine engines are used in a broad spectrum of aeronautical applications including helicopters, commuter and general aviation aircraft, and cruise missiles. Large engines have been made significantly more efficient through component and material advances and high compressor pressure ratios. These technology improvements are not directly transferable to small engines, however, because of adverse scaling effects and differing turbomachinery types—radial instead of axial. For example, current 500-hp turboshaft engines are about 35 percent less efficient than their large counterparts, and this restrains the capabilities of small aircraft.

Recent in-house analyses examined the opportunities offered by advanced thermodynamic cycles, turbomachinery components, and high-temperature materials. Adding a lightweight, compact heat exchanger to an advanced turbomachinery engine in order to recover some of the normally wasted exhaust heat (i.e., regenerative cycle) could reduce fuel burned by 55 percent and direct operating costs by 25 percent. Attainment of such advanced propulsion technologies would enable revolutionary improvements in aircraft capabilities and economics. □

Altitude Wind Tunnel

Modern Turning Vanes for Wind Tunnels

Lewis is studying a potential rehabilitation of the Altitude Wind Tunnel (AWT) to make it a unique national subsonic (Mach 0.1 to 1.0) propulsion, icing, and aeroacoustic facility. As a result of retaining the major geometric features of the original tunnel while increasing the maximum Mach number of the test section from 0.6 to 1.0, the flow velocity into each of the four corners is now higher. For the corner downstream of the test section the velocity is about three times greater than the conventional design value. Since the total pressure loss for any given tunnel circuit component tends to increase with the square of the velocity entering the component, and since it is desirable to minimize pressure losses in order to reduce tunnel power and cooling requirements, it was mandatory that the AWT corners be designed to keep total pressure losses as small as possible.

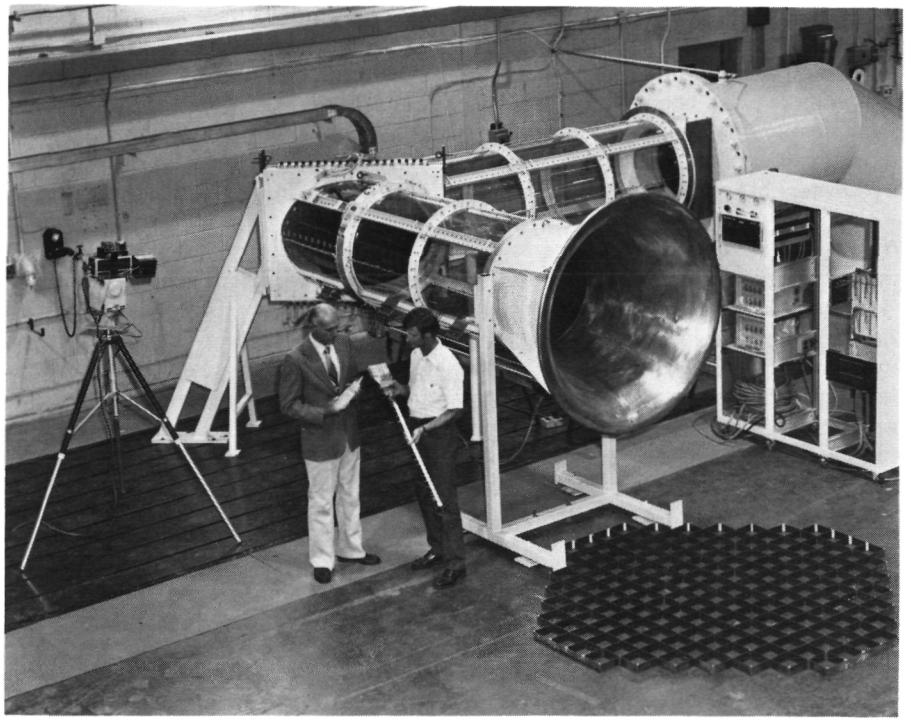

AWT corner-turning vane test

To accomplish this, an inverse design method was used to develop a new corner-turning vane shape. The vane surface velocity distribution for minimum loss was specified, and the vane shape needed to provide that distribution was determined. One-tenth scale models of the corners were then built and tested. The corner downstream of the test section showed on overall corner loss that was about 15 percent lower than that of the same corner with conventionally shaped turning vanes. This reduction in corner loss represents a significant reduction in overall circuit losses and ultimately will signficantly lower power and cooling requirements. □

Real-time multiprocessor simulator

Real-Time Multiprocessor Simulator

Lewis has developed a low-cost, easily programmed computing system that can simulate complex dynamic systems in real time. The essence of the system is a network of computers tied together and operating simultaneously, each performing a portion of the overall simulation task. The use of multiple computers increases computing speed relative to a single computer. By operating in real time the simulator can be used for hardware-in-the-loop testing of controls and for pilot-in-the-loop studies.

Using state-of-the-art, high-performance microcomputers, Lewis engineers have designed, built, and tested a six-computer experimental simulator. A mathematical model of a gas turbine engine has been used as a benchmark. The multiprocessor configuration can be expanded to handle more complex simulations. In addition to the simulator hardware, Lewis has also developed powerful software packages that make it easy for those who are not computer specialists to program and operate the multiprocessor system. One such package is a generic, high-level programming language code for a variety of popular microprocessors. Future applications of the multiprocessor simulator will include the simulation of the Lewis Altitude Wind Tunnel (AWT) and the evaluation of new AWT control designs. □

Aeronautics

Title	Lewis contact	Telephone number, (216) 433–	Headquarters program office
Instruments and Controls:			
Advanced Sensor Failure Detection for Aircraft Engine Controls	Walter C. Merrill	3748	OAST
Systems for Whole-Field Flow Measurement	Arthur J. Decker	3639	OAST
High-Power Arc Lamp for High-Heat-Flux Experiments	Curt H. Liebert	3726	OAST
Internal Fluid Mechanics:			
Modeling the Internal Combustion Engine	Bonnie J. McBride Frank J. Zeleznik	5870 5912	OAST
Turbulent Boundary-Layer Separation and Reattachment	Donald M. Sandercock	5855	OAST
Heat Transfer in Heat Exchanger Passages	Robert J. Boyle	5889	OAST
Propulsion Systems:			
Ceramic Matrix Combustor Liner	Carl T. Norgren	3392	OAST
Airfoil Performance in Icing	Robert J. Shaw	3942	OAST
Ceramic Rotary Engines	Edward A. Willis	3401	OAST
Ceramic Component Technology for Low-Heat-Rejection Diesel Engines	Robert C. Evans	3401	OAST
Ceramic Component Technology for Gas Turbine Engines	Robert C. Evans	3401	OAST
Successful Demonstration of Convertible Engine	Kaleel L. Abdalla	3961	OAST
Structural Integrity of Advanced Propfans	Oral Mehmed	6036	OAST
Modeling of Profan Inlets	John B. Whitlow	3936	OAST
Performance of Counterrotation Propeller Models	John E. Rohde	3949	OAST
Vibratory Response Test of Fairey-Gannet Counterrotation Propellers	Irving E. Sumner	3930	OAST
Propfan Acoustic Model Tests	Eugene A. Krejsa	3952	OAST
Advanced Small-Engine Technology	Calvin L. Ball	3397	OAST
Regenerative Engine Cycles	William C. Strack	5634	OAST
Altitude Wind Tunnel:			
Corner Turning Vanes for New Altitude Wind Tunnel	Franklin J. Kutina, Jr.	3424	OAST
Real-Time Multiprocessor Simulator	Franklin J. Kutina, Jr.	3424	OAST

Space Propulsion Technology

Centrifugal Pumps for Low-Thrust Rockets

Pump-fed, low-thrust chemical propulsion systems are being considered for transferring acceleration-limited structures from low Earth orbits to geosynchronous or other high Earth orbits. Engine systems for these applications will require low-flow-rate, high-head-rise pumps that fall outside the design range of existing rocket engine turbopumps. The low flow rate (2 to 16 gal/min for oxygen and hydrogen propellants) calls for impeller diameters of about 2 inches and hydrodynamic passage heights as small as 0.030 inch. Flow can also be reduced with somewhat larger passage heights by blocking diffuser passages (partial emission) or impeller passages (partial admission), but these concepts have not been used in the size under consideration.

A technology program that addresses the producibility and performance uncertainties associated with this new class of pumps is being conducted by Rocketdyne under contract to Lewis, with a portion of the work done under Rocketdyne-funded tasks. Six types of centrifugal pump stages encompassing the key design concepts and features applicable to low-flow-rate pumps have been fabricated and tested in water. Precision investment casting was shown to be a viable process for fabricating shrouded impellers with passage heights as small as 0.030 inch. The comprehensive water-test data base enables knowledgeable decisions to be made on this concept in future low-thrust engine programs and provides factual data for engine system analyses. □

Turbine Loss Analysis

The space shuttle main engine (SSME) is a high-performance, liquid-propellant (hydrogen-oxygen) rocket engine. The high performance is attained by using a staged-combustion power cycle coupled with high combustion chamber pressure. The propellants are burned in preburners to produce hydrogen-rich gas (steam), which in turn powers the high-performance turbopumps. Large aerodynamic losses must be compensated for by increasing the turbine inlet temperature in order to achieve the required power. Higher turbine inlet temperatures shorten the life and reduce the durability of the engine.

Losses in the high-pressure fuel turbine (HPFT) and the high-pressure oxidizer turbine (HPOT) at full power were assessed by using a quasi-three-dimensional flow and boundary-layer analysis. The results were used to calculate blade and end-wall friction losses and trailing-edge mixing losses. Additional empirical correlations were used to calculate losses due to rotor tip clearance, incidence, secondary flow, and rotor blade surface roughness. The calculations were made at Reynolds numbers equal to those in the engine.

The HPFT had a calculated overall two-stage efficiency of 85.2 percent. A 5-point efficiency loss was attributed to rotor blade surface roughness due to the nickel-chromium-aluminum-yttria (NiCrAlY) coating that had been plasma sprayed on the blade. The surface roughness was measured as 250 microinches root mean square. The root tip clearance loss, the next most significant loss for the HPFT, accounted for 4 points. The HPOT had a calculated overall two-stage efficiency of 80.1 percent. An 8-point efficiency loss was attributed to rotor incidence and a 6.3-point loss to profile and mixing effects.

The HPFT losses could be reduced by modifying the existing blading to improve the surface finish to approximately 32 microinches. The HPOT would require redesign of the blading to reduce the losses. Reducing either the HPFT or HPOT losses could significantly extend turbine life by allowing a reduction in turbine inlet temperature. □

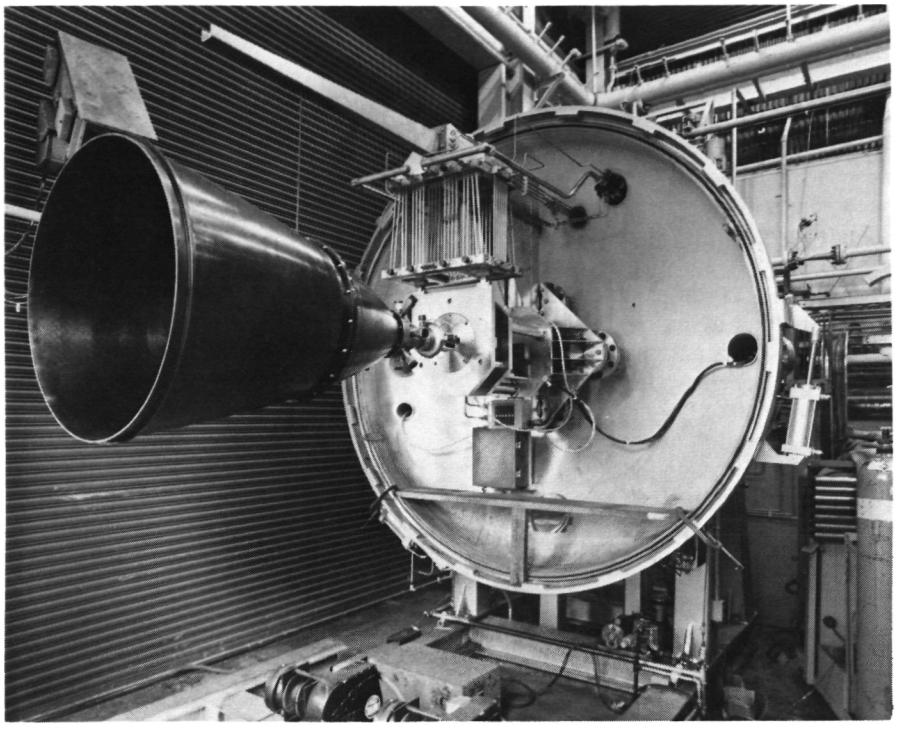

Thrust stand with 1000-area-ratio nozzle

Altitude Capability at Rocket Engine Test Facility

Maximizing the performance of advanced rocket propulsion systems requires special-purpose nozzles much larger in area ratio than current nozzles. Future space engines could require nozzles with an area ratio of 1000 or larger; in comparison the area ratio of the Centaur engine is only 57 and that of the space shuttle main engine only 77. These space engines must also be compact to conserve volume within the cargo bay of the space shuttle.

Recent attempts to design such nozzles has revealed uncertainties in the computerized models: performance differences of 15-sec impulse at an area ratio of 1000 resulted from different prediction techniques. Obviously these technologies are beyond the state of the art and require experimental tests to help develop the concepts and to validate improved computer models. These tests must be conducted in a simulated space environment to determine nozzle performance.

Until the Rocket Engine Test Facility (RETF) at Lewis became operational with a full range of propellant capabilities, no facility was available to test 1000-area-ratio nozzles with cryogenic propellants. Driven by high-pressure fluid systems, the components can be tested without the need for turbomachinery or supporting systems to simulate inlet conditions. That high-pressure fluid source is the backbone of the system. An existing test position designed for smaller thrusters was modified to accommodate the new capability. The existing high-pressure fluid systems were employed to drive several arrangements of ejectors to pump down a test capsule with the engine installed. A self-pumping, zero-flow, cooled diffuser was fabricated to use the rocket engine energy for additional pumping. Space simulation for starting was provided by connecting with a house vacuum system at the RETF.

By operating the rocket combustion chamber at pressures to 2000 psia, nozzle pressure ratios can be achieved that will allow testing of 1000-area-ratio nozzles. The full range of safe fluid-handling capability allows testing with hot-gas systems such as hydrogen-oxygen or with cold, noncondensing fluids such as pure hydrogen. The latter capability will be used to isolate some of the variables in nozzle studies by eliminating combustion- or high-temperature-induced problems.

High-area-ratio nozzles and associated combustion devices are on hand. The initial research tests with the facility will attempt to demonstrate its maximum capability with 1000-area-ratio nozzles. □

Compatibility of Grain-Stabilized Platinum with Resistojet Propellants

Resistojets provide thrust by passing a propellant through an electrically powered, resistively heated, high-temperature heat exchanger and expanding the propellant through a nozzle. The resistojet is a candidate for space station auxiliary propulsion because of its promise of long life and its potential for using any of the many propellants that will be available. The resistojets ability to satisfy the demanding requirements of long life and multipropellant capability are, however, limited by the available materials.

A series of experiments were conducted to determine the lives of grain-stabilized platinum-yttria (Pt/Y_2O_3) and platinum-zirconia (Pt/ZrO_2) and their compatibility with carbon dioxide (CO_2), methane (CH_4), hyrodgen (H_2), and ammonia (NH_3). All samples were resistively self-heated, and each was exposed to one of the flowing gas environments for 1000 hours. The changes in material surface and mass were used as indicators of compatibility and life.

The Pt/Y_2O_3 and Pt/ZrO_2 samples exposed to CH_4 and CO_2 showed negligible surface changes; the samples exposed to H_2 and NH_3 showed evidence of minor surface corrosion. All of the samples showed small amounts of grain growth. These surface changes and slight grain growth are not, however, expected to significantly affect the performance of a resistojet made of these materials. The low mass losses indicated that both Pt/Y_2O_3 and Pt/ZrO_2 would maintain their integrity in each propellant environment for more than 200 000 hours.

As a consequence of these tests grain-stabilized platinum has been selected for the multipropellant resistojet presently under development as a candidate for space station auxiliary propulsion. □

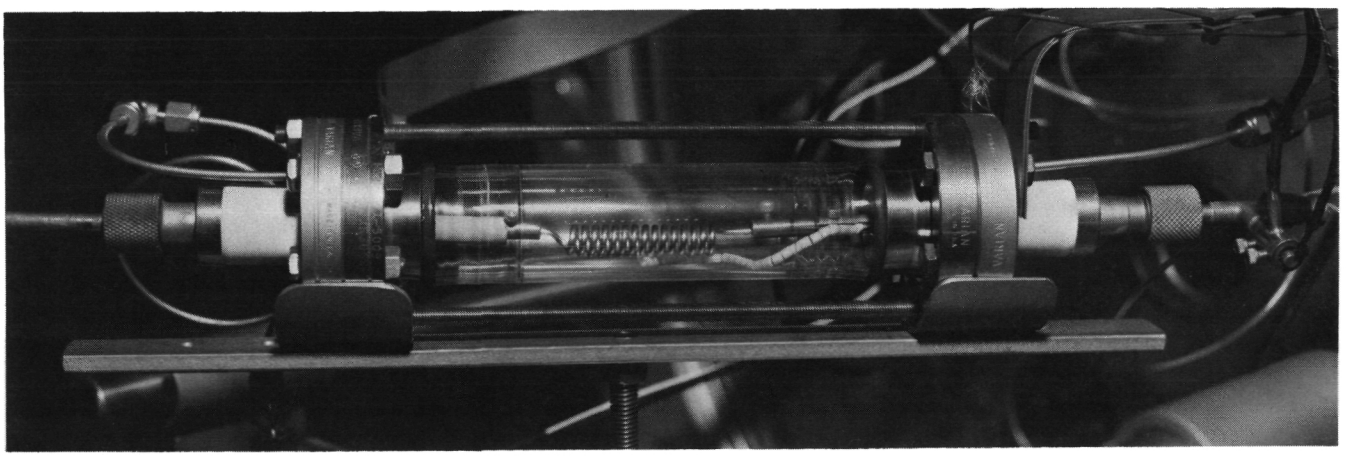

Resistojet materials test cell

Rail Accelerators

The functional mechanisms of rail acceleration have been evaluated at Lewis in order to assess its potential for Earth launch of heavy, nonfragile payloads. One-meter-long accelerators with bores of 4×6 mm and 12.5×12.5 mm were tested in a 240-kJ pulsed power facility. In normal operation an arc is struck between metallic rails, accelerates along the rails, and imparts a force to a projectile that is thereby accelerated. An accelerator design was used that enabled, for the first time, the use of streak photography to observe the plasma behind the projectile. The plasma often decoupled from the rear of the projectile, resulting in loss of projectile acceleration and therefore a lower final velocity. This behavior is thought to be due to evaporation of the rail surfaces, which adds mass to the plasma and thus slows it. This phenomenon was subsequently used to explain rail accelerator performance at five other national and contractor laboratories. □

High-Power Xenon Ion Thruster

The projected need for higher levels of space power has stimulated strong interest in ion thrusters operating at high power levels on inert gaseous propellants such as xenon. Such thrusters would be much lighter than the previously developed 3-kW mercury thrusters, and the propellants are nontoxic, noncontaminating, and nonreactive with ground and space systems. Therefore a 30-cm-mercury thruster was modified and tested with xenon propellant.

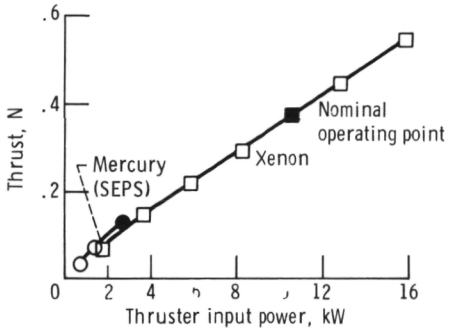

Thrust versus ion thruster input power

The xenon thruster produced four times the thrust of the mercury thruster (0.12 lb versus 0.03 lb) at six times the power. Based on a preliminary assessment 10.6-kW power and 0.08-lb thrust was selected as the operating point at which the 30-cm-thruster would be expected to have a useful lifetime. These demonstrated increases in power and thrust cut the ion propulsion system specific mass by more than one-half and make ion propulsion a more attractive candidate for high-power missions. □

Low-Power Direct-Current Arcjet

The direct-current arcjet is currently being considered for auxiliary propulsion. In these devices an arc is struck between a cathode and an anode. The propellant is heated in a long constrictor between the electrodes and then expanded in a nozzle. If they are to be used on geosynchronous satellites, however, arcjets must operate at power levels of 1 kW or less as well as have long life and higher efficiency. Prior work indicated that arcjets become unstable below about 1.5 kW. To evaluate low-power arcjets, a modular, water-cooled, arcjet simulator was developed.

Using a vortex propellant flow field and optimizing the constrictor diameter and length and the cathode-to-anode spacing led to a stable operating envelope extending to below 0.5 kW. Additionally the use of a vortex flow field allowed containment of the arc and appeared to greatly reduce or eliminate erosion of the cathode and other thruster components. Finally calorimetric data verified efficient transfer of arc energy to the propellant as only 20 to 30 percent of the input energy was deposited at the electrodes, even under water-cooled conditions.

Vortex-flow-field arcjets using storable propellants are now thought to be viable candidates for near-term auxiliary propulsion for Earth orbital spacecraft. □

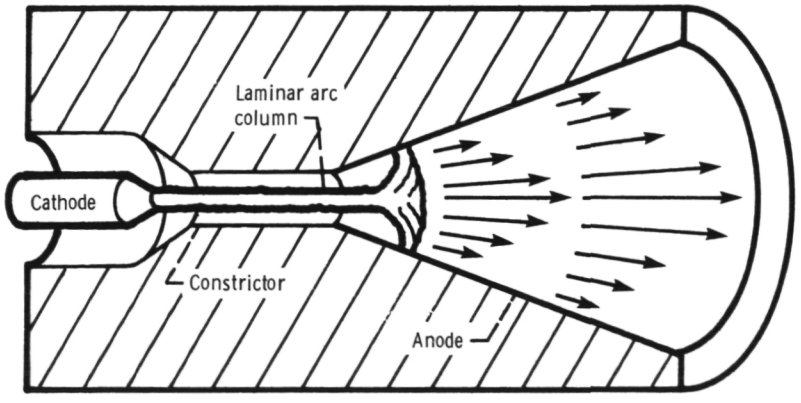

Arcjet fundamentals

Tungsten-Reinforced Copper Thrust Chamber Liner

The inner wall liners of reusable rocket thrust chambers that operate at high chamber pressures are fabricated from materials of high thermal conductivity and high strength. Presently the liners are fabricated from high-strength copper alloys capable of transmitting the high heat load from the hot-gas-side wall to the coolant and of carrying the high pressure loads. However, the severe environment causes an irreversible plastic deformation of the cooling passage wall during each firing cycle. Repeated cycles cause cracks in the wall that limit the life of the thrust chamber.

Using a composite material for the liner, tungsten wire in a copper matrix, offers the potential for extending thrust chamber life. The tungsten wire has the high strength necessary to carry the pressure loads and to prevent deformation of the cooling passage wall; the copper has the high conductivity necessary to transmit the heat load to the coolant. The tungsten-copper composite, with only a 10 percent volume of tungsten, has nearly double the strength of present high-strength copper-base alloys with only slightly less thermal conductivity.

Fabrication consists of spraying a layer of liquid copper onto a steel mandrel that has the desired shape of the thrust chamber liner. Tungsten wire is then wrapped over the copper, and a second layer of copper is applied in sufficient thickness to permit the machining of the cooling passages. Intermediate steps consist of hot isostatic presses to densify the copper and to ensure intimate contact between the wire and the copper matrix. After the cooling passages have been machined, the mandrel is removed and the fabrication is completed conventionally. Fabrication feasibility has been demonstrated for both cylindrical and contoured rocket thrust chamber liners. □

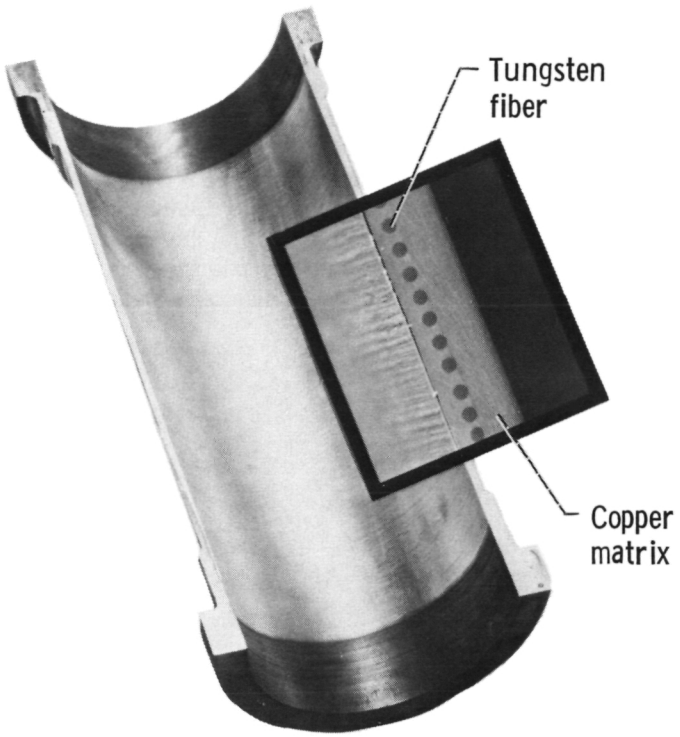

Construction of tungsten-reinforced copper thrust chamber liner

Composite Materials for Rocket Nozzles

Regeneratively cooled liquid-propellant rocket engines (i.e., having cooling propellant flowing through tubes that make up the walls of the basic chamber-nozzle combination) generally give high performance and are presently used as powerplants for both boost and upper stage vehicles. Future space missions, however, will require performance increases over even the present high values. One way these increases can be attained is by elongating the nozzle (the funnel-shaped section of the engine located downstream of the combustion chamber) to provide more surface area for the expanding combustion gases to push against.

Nozzles are generally elongated by adding additional sections (called secondary nozzles) either singly or in tandem until the overall engine size is achieved. Any added nozzle sections are usually cooled only by radiation and hence will necessarily operate at higher temperatures than the regeneratively cooled wall of the basic engine. Any secondary nozzle section adds length to the engine system, and since payload space must not be jeopardized, the section is generally stored in telescope fashion until the engine is to be fired. When needed, it is slid into position and secured.

For some applications secondary nozzles have been constructed of special metals. Use of carbon-carbon composite materials, however, would represent a significant weight saving and hence an increase in payload allowable weight. Under Lewis' direction the Pratt & Whitney Aircraft Company built two 20-inch-long carbon-carbon composite nozzles for testing on the Lewis-managed oxygen-hydrogen RL10 rocket engine. The nozzles were representative of the two major fabrication processes in everyday industrial use. Each nozzle also was covered with a thin protective coating of silicon carbide.

These nozzles were tested successfully as apart of an RL10 engine system in an altitude facility at the contractor's plant. The nozzle ran for a total of almost 80 min over 41 different run periods. During these tests the analytically predicted improvement in engine performance was verified. This work has shown that coated carbon-carbon composite is a viable material for hydrogen-oxygen rocket engine nozzle extensions and can increase the allowable payload weight. □

Power Technology

Improved GaAs Concentrator Solar Cell

Under a Lewis contract to develop a gallium arsenide (GaAs) concentrator solar cell, Varian Associates has produced several cells with conversion efficiencies of over 21 percent at a solar concentration of 100 and a temperature of 80 °C. This is an improvement of 2 percentage points over the 19-percent efficiency previously obtained by other researchers and approaches the practical limit of about 23 percent. Improvements were made in the antireflection coating and the top grid contact pattern. The cells are made by using an epitaxial growth method, which allows a wide variation in cell geometry and material parameters.

These concentrator cells are prime candidates for use in a miniature Cassegrainian collector under development by NASA. The Varian GaAs cells will improve array output by a least one-third over current flat-plate silicon cell arrays. □

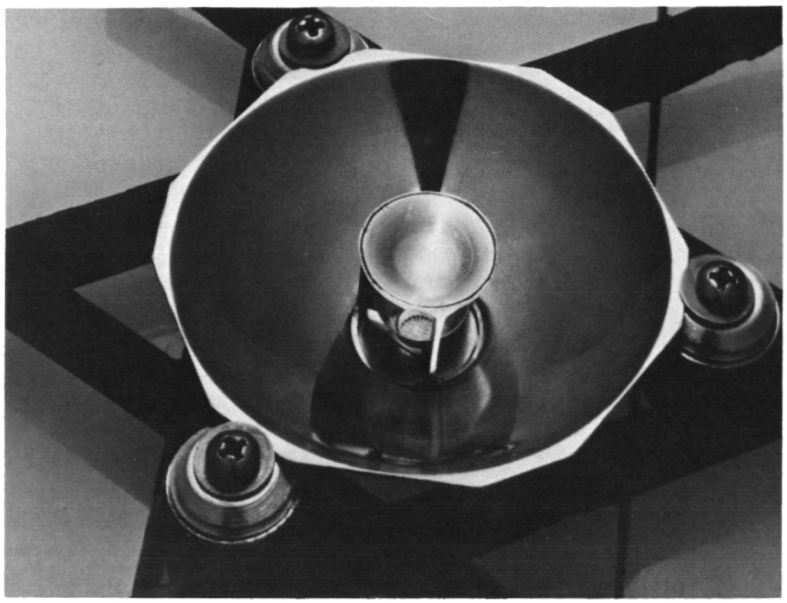

Miniature Cassegrainian concentrator element

Protective Coatings for Spacecraft Polymers

Early space shuttle flights have demonstrated that Kapton is gradually eroded and suffers changes in optical properties when exposed in low Earth orbit. The rates of material loss have been sufficiently high to potentially compromise the long-term durability of solar arrays or thermal blankets using Kapton. The postulated mechanism for material loss is oxidation by ram impact of the geosynchronous atomic oxygen that dominates the low Earth orbital environment at altitudes between 97 and 351 miles.

An approach to preventing oxidation is to use a protective barrier. Such a barrier, or coating, must itself be unaffected by atomic oxygen bombardment. In addition, the coating should be flexible, thin, lightweight, adherent, tolerant to ultraviolet radiation, and abrasion resistant. It must also not alter the substrate's optical and adhesive bonding properties if it is to be used for protecting polymers such as Kapton. Thin film coatings of predominantly metal oxide with small amounts of fluoropolymer for flexibility have been shown in both ground and space shuttle testing to protect Kapton from atomic oxygen. These coatings, developed at Lewis, were produced by ion beam sputter codeposition of a metal oxide and a fluoropolymer target.

The films, only 60-nm thick, are mostly silicon dioxide (SiO_2) with a small volume fraction (4 to 15 percent) of polytetrafluoroethylene. They are flexible enough to protect Kapton solar array blankets, the hinge portion of which may need to be bent to a 0.6-mm radius of curvature without coating failure. The films are more flexible than pure SiO_2 films without sacrificing atomic oxygen protection capability. □

Space Station Environmental Compatibility

Interactions between the space station and its orbital environment can significantly affect its operation, lifetime, and safety. Interactions with orbital particle and field environments are important for any space system. Radiation damage and aerodynamic drag, for example, must be considered in designing any flight system. However, a number of interactions become important design considerations for a large, high-power, long-life system such as the space station.

The space station's power requirements dictate higher voltage solar arrays and power distribution than have been flown to date. Higher voltages lead to increased interactions with the electrically charged ionospheric plasma. These interactions could result in operational and safety hazards to the entire system if not considered in the design. The large size of the system and its long lifetime requirement also present new environmental compatibility problems to the designer. Lifetime poses a particular challenge in selecting materials because of the recently discovered vulnerability of many common spacecraft materials to erosion by the residual atmosphere, whose main constituent at space station altitudes is monatomic oxygen.

To assist space station designers in developing an environmentally compatible operational system, members of the Lewis staff have compiled a document entitled "Environmental Interactions Considerations for Space Station and Solar Array Design (Preliminary)." The document contains the results of an NASA/Air Force program established in 1981. It summarizes the current understanding of environmental compatibility considerations in a form useful to space station designers.

The document is divided into four parts. The first introduces interaction concepts. The second details modeling techniques for assessing a design and their state of development. The third focuses on critical design issues for the space station as a whole, the power system, and the solar array itself. The fourth summarizes the program recommended to obtain additional information required to resolve space station design issues. A bibliography is provided for those desiring further information on specific topics. □

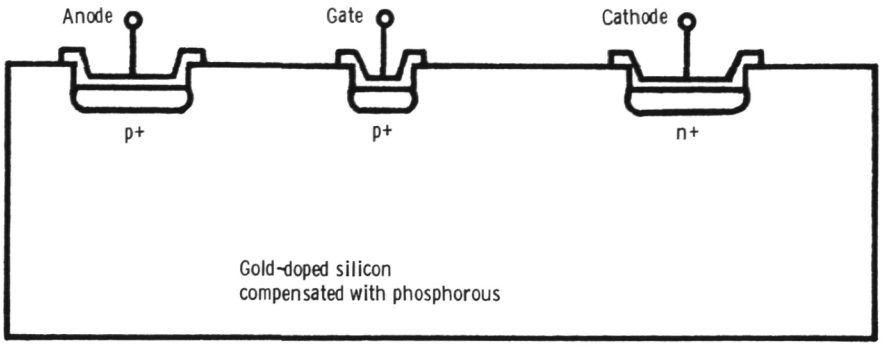

Cross section of typical double-injection semiconductor

High-Power Linear Amplifier

Alternating-current power sources capable of providing variable frequency up to and beyond 20 kHz, controllable output voltage, and both sinusoidal and nonsinusoidal waveforms are required for testing high-power, high-frequency space components. These tests are necessary to determine the performance characteristics of newly developed space components such as transformers, capacitors, and transmission lines. A versatile ac power source with these capabilities is a linear amplifier in conjunction with a waveshape generator.

A 2.5-kW audiofrequency linear amplifier has been developed under Lewis sponsorship by Northam Electronics, Inc. The amplifier has a peak-to-peak voltage output of 460 V and can deliver 20 A of peak current. Because almost any waveshape can be used as an input, a wide variety of high-power components can be tested under the same waveshape and voltage as will be used in the circuit. Although the basic module is 2.5 kW, higher power or higher voltages and currents can be obtained by series or parallel operation. □

New Semiconductor Family

A new family of semiconductor devices has been developed that is based on double-injection techniques and compensated deep impurities in silicon. These devices hold great promise for switching high power at voltages exceeding 20 000 V in space environments of high temperature and radiation. The new semiconductors may be used in power processing and control of space nuclear energy sources, high-intensity lasers, space-based radar, high-power communications tubes, and various unique types of sensors and transducers. While extending voltage, temperature, and radiation limits well beyond those of conventional semiconductors, the devices provide important enabling technology for NASA's growth space station, SP–100 program, and advanced lunar bases and for the President's Strategic Defense Initiative.

Several gating schemes provide improved switching efficiencies, delay properties, and sensing applications over conventional semiconductors at both high- and low-power logic levels. In addition, several potential spinoff transducer and sensor devices that use this semiconductor technology are being investigated at the University of Cincinnati for critical applications in medicine, life support, and industrial processes and equipment. □

Radiation Resistance of Power Switches

One of the more radiation-sensitive components in space nuclear power systems of the future will be the solid-state switches required for power, protection, and control circuits in space electrical systems. Lewis is conducting a program to investigate how gamma rays and neutrons affect the performance characteristics of high-power transistor switches. Nine types of high-power transistor switches have been irradiated with gamma rays to a cumulative dose level of 1 megarad. The gamma facility at Sandia National Laboratory was used to irradiate the switches, and the recently completed high-power-transistor analysis laboratory at Lewis was used to conduct the electrical performance tests after each successive level of irradiation. Results to date show some degradation in electrical performance characteristics of the transistor switches, but no catastrophic failures have occurred at the present cumulative dose level of 1 megarad. Surprisingly, some characteristics were actually improved by irradiation. □

Analysis of Radiation-Cooled Transmission Lines

As space power levels rise to meet mission objectives and transmission distances between power sources and loads get longer, the mass, volume, power loss, and operating voltage and temperature of the transmission line become important system design considerations. Lewis has analyzed advanced transmission lines for large space power systems such as advanced space stations, lunar bases, and the SP–100 program.

In these analyses the transmission lines not only transmit the power, but also act as their own radiators by directly radiating to space the electric power losses generated within the conductor material. This study clearly indicates that in future large space power systems the transmission line weights and losses will be important. The study also shows that transmission line voltages will need to be much higher, in the range of 1000 V. □

Simulation of Integrated Coal Gasifier/Fuel Cell Powerplants

Under contract to Lewis, a Cleveland State University research associate has developed several codes to simulate the performance of integrated coal gasifier/phosphoric acid fuel cell (PAFC) powerplants. One system study used the Texaco gasifier and the United Technologies PAFC system. The Texaco gasifier was chosen from those gasifiers that are commercially available. Its system efficiency of nearly 40 percent exceeds conventional utility powerplant efficiencies of around 30 percent.

Another system study used the TRW catalytic hydrogen system, which is in development. This system attained an efficiency of 46 percent. Sensitivity studies and tradeoff analyses were performed on each system with various operating parameters (e.g., utilization of fuel and oxidant in the PAFC and operating current density). The results of these parametric studies showed an improvement in the system performance efficiency and a reduction in the cost of electricity for each system. □

Fuel Cell Electrode Modeling

Under a Lewis advanced research contract to investigate electrode structures for phosphoric acid fuel cells, Stonehart Associates, Inc., has developed computer software for a mathematical theory of mass transport of reactants in porous gas diffusion electrodes. In the theory a simplified model for the electrode structure is used and fitted to experimental data. The specialized application of this model for low reactant concentrations allows a quantitative evaluation of important mass transfer processes in fuel cell electrodes; this should prove useful in controlling electrode development and improving performance. □

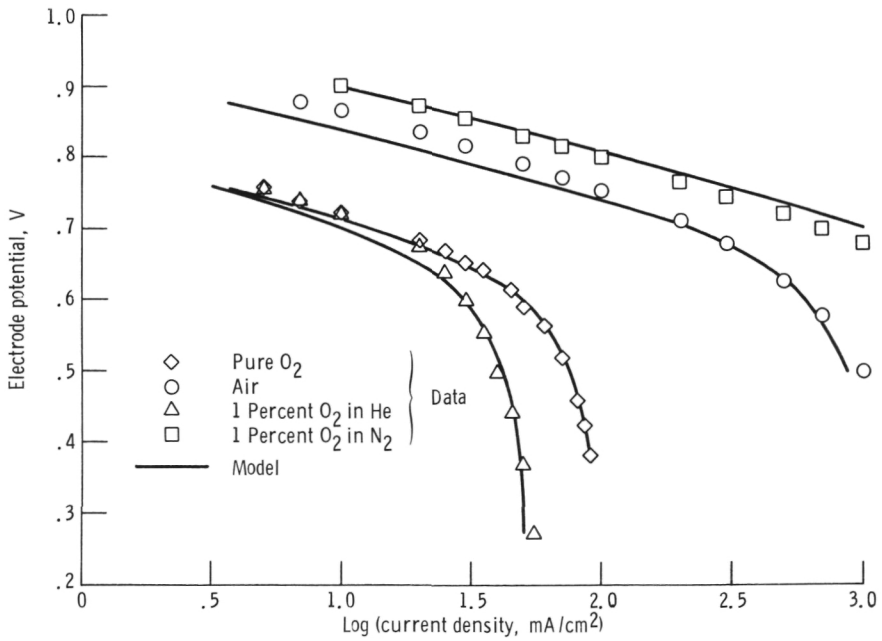

Electrode performance

Free-Piston Stirling Engine for Space Power

Lewis is evaluating the free-piston Stirling engine for space power applications in support of the SP–100 program. The Department of Defense, the Department of Energy, and NASA jointly fund SP–100 to develop a 100-kW class electrical space power module. The potential advantages of free-piston Stirling engines for space application include high efficiency, potential long life and high reliability, no dynamic seals, extremely low vibration, simple components, and growth capability.

As part of the SP–100 program Mechanical Technology Inc. has designed, fabricated, installed, and successfully conducted initial testing on a nominal 25-kW, two-opposed-piston Stirling engine/linear alternator system in less than 16 months. The space power demonstrator engine (SPDE) is about 1¼ m long and about 1/3 m in diameter. The engine was suspended from the ceiling by four straps during testing, and no discernible vibration was observed. During initial shakedown testing this engine produced about 4 kW at reduced pressure and frequency conditions. This level is the highest power achieved for a designed-for-space free-piston Stirling engine/linear alternator device. Once the low-power data are analyzed, the engine will be run at design pressure and frequency.

The SP–100 Stirling activities, of which the SPDE is a major part, have demonstrated that

- Stirling engine/linear alternator systems can be scaled
- Hydrostatic and hydrodynamic gas bearings with long life potential can be used for Stirling engine/linear alternator systems
- Performance at low engine temperature ratios (~2) can be achieved
- Opposed-piston engines provide excellent dynamic balancing capability
- Low-specific-weight engines can be built and successfully run

In addition, Mechanical Technology Inc., under a cooperative funding arrangement with the SP–100 program office and the Gas Research Institute, has demonstrated more than 5000 hours of endurance testing without component failure on a 2-kW free-piston Stirling engine/linear alternator system. Tests are continuing. □

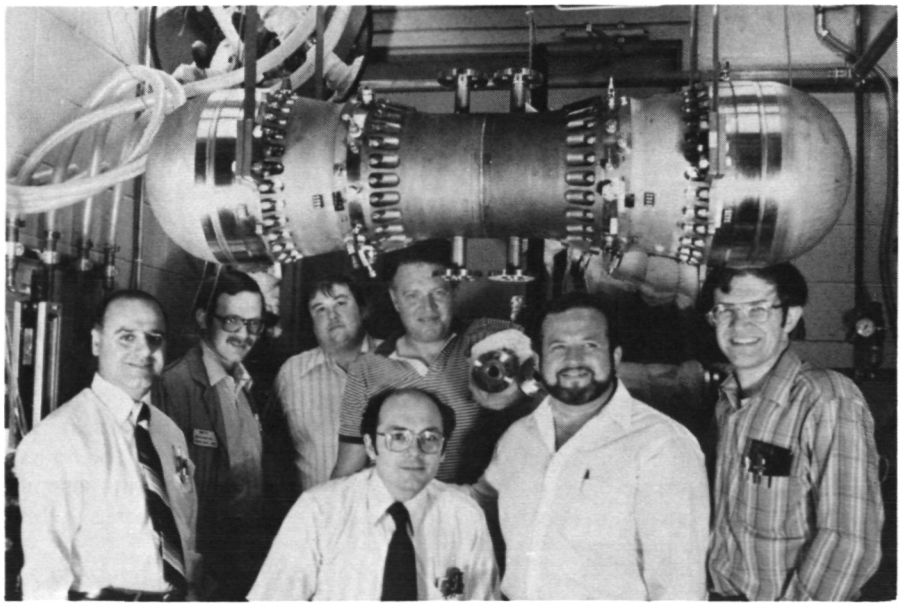

Free-piston Stirling engine

Second-Generation Automotive Stirling Engine

The Stirling engine is being developed as a possible alternative to the spark-ignition engine under the Department of Energy's Highway Vehicle System program. Lewis manages the Automotive Stirling Engine (ASE) project. Mechanical Technology Inc., the prime contractor, has designed and built seven experimental first-generation (Mod I) engines that have accumulated over 13 000 hours of operation. The Mod I engines are now being used to develop and demonstrate new technologies for a second-generation engine, the Mod II. The Mod II engine is expected to demonstrate the ASE project goals in an engine/vehicle system in September 1987.

The detailed design of the Mod II Stirling engine system, which includes all the auxiliaries and controls, was completed in 1985. The Mod II is rated at 62.3 kW (83.6 hp) and has an operating temperature of 820 °C. It contains an equal-angle V-drive system, an annular heater head, a rolling-element drive unit, a metallic preheater, a simplified combustor, a lightweight piston rod unit, and a simplified auxiliaries and control system. Procurement of the long-lead-time hardware for two Mod II ASE's was started in 1985.

The ASE program goal is at least 30 percent better fuel economy than a comparable spark-ignition-powered vehicle and performance equal to, or better than, that of a comparable vehicle. The Mod II is projected to have a combined mileage of nearly 41 mpg and an acceleration time of less than 13 sec (0 to 60 mph) when installed in a General Motors Celebrity vehicle in the 3125-lb inertia weight class. The Mod II fuel economy is projected to be 50 percent above the U.S. fleet average for this weight class. The ASE program, with the Mod II Stirling engine, is expected to meet or exceed its goals by September 1987. □

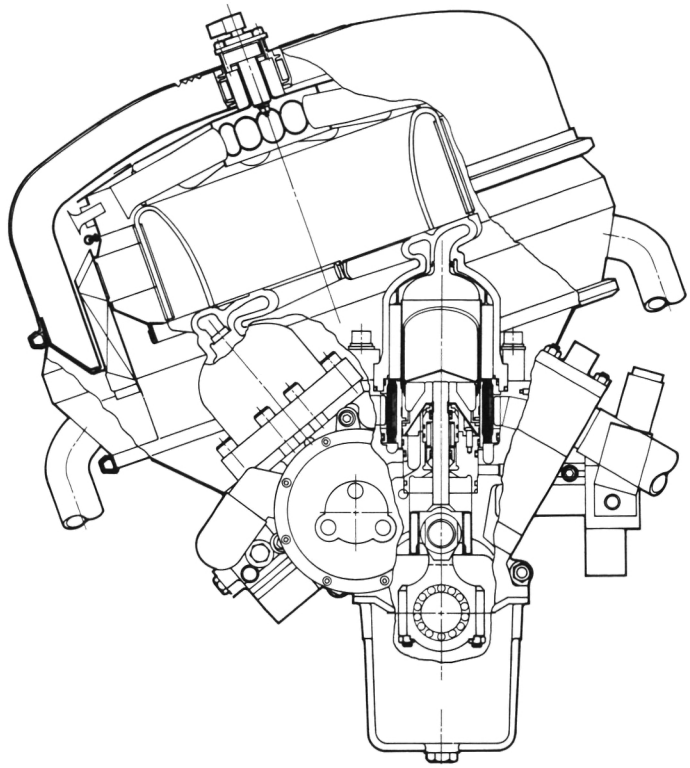

Automotive Stirling engine

Bipolar Nickel-Hydrogen Batteries

Technology for an actively cooled, bipolar nickel-hydrogen battery system is being developed in-house and on contracts with Ford Aerospace and Yardney Electric. Preprototype stack hardware has been assembled and tested to demonstrate the weight, volume, and performance advantages of this concept. These battery systems will be particularly applicable to situations requiring high voltage and high power peaks. An experimental 10-cell stack with a nominal output of about 500 W, a peaking capability of about 10 kW, and a nominal capacity of 50 A-hr has been assembled. The 8- by 24-inch cell is cooled by circulating a coolant through five thin plates placed between a pair of cells.

The contractor team has operated a 10-cell actively cooled design verification stack (4 by 8 in.) and is constructing its first article for cycle life testing. The test article is 4 inches by 4 ft and will have a nominal capacity of 75 A-hr. □

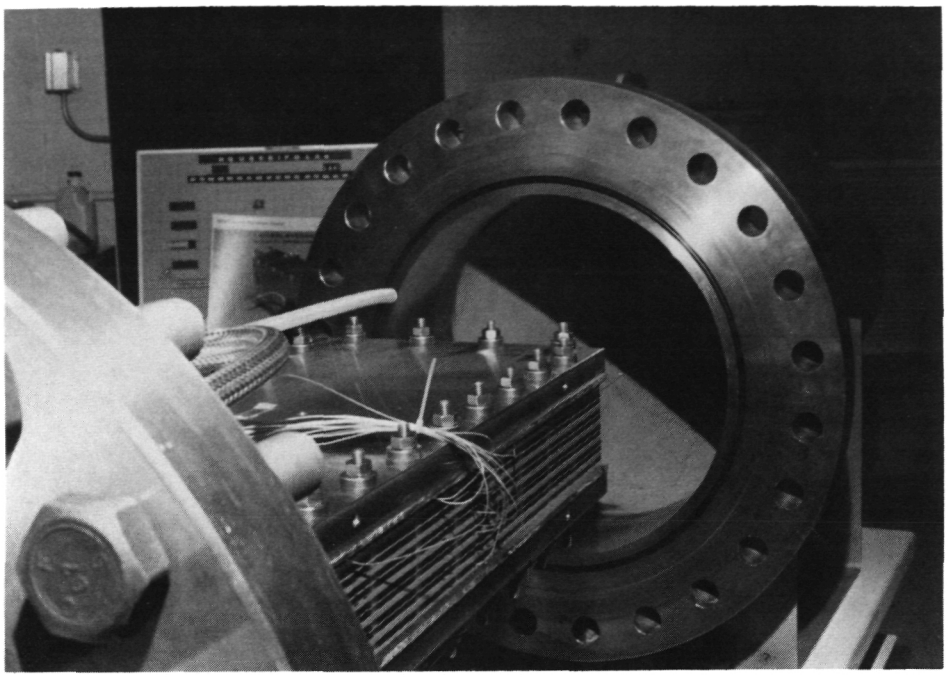

Experimental 10-cell bipolar nickel-hydrogen battery stack

Advanced-Design Nickel-Hydrogen Cells

Individual-pressure-vessel (IPV) nickel-hydrogen cell designs have been developed for upcoming low-Earth-orbit missions. These cells are adaptations of cell designs developed for geosynchronous applications. Several novel features are intended to circumvent some of the performance decay modes in state-of-the-art IPV cells. These novel features are based on the best available understanding of cell operation. Experimental cells that incorporate these features are being tested with encouraging results. Eagle Picher Industries, General Electric, Yardney Electric, Ford Aerospace, and the Air Force are considering adapting several of these features for their own advanced cell designs. □

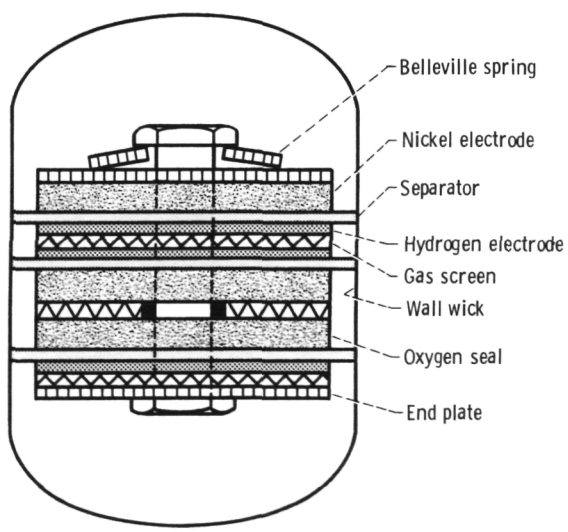

Advanced-design IPV nickel-hydrogen cell

Structures

Vibratory Characteristics of Advanced Turboprops

An experimental program was carried out to develop a structural dynamic data base for swept turboprops. Data were gathered in a series of evacuated spin tests to 9000 rpm. Steady-state blade deformations under centrifugal loading as well as vibratory characteristics of the rotor assembly have been measured and compared with analytical values. Several unique measurement and excitation techniques were used.

The steady-state deformations were determined by measuring the angular deflections of a laser beam reflected from mirrors bonded to the blades. In addition, tip deflection was measured directly with high-speed strobe photography. The blades were excited with a piezoelectric crystal system in which standing or traveling waves could be generated. Advanced data reduction procedures were used to provide deformation, mode shape, and frequencies of the turboprop assembly.

Significant differences were noted between calculated vibratory stress distributions and corresponding measurements for the third, fourth, and fifth modes of vibration. Modes 1 and 2 showed satisfactory agreement. The calculated blade tip axial deflection agreed well with the measurements, but significant differences exist for the untwist and uncamber deflections. □

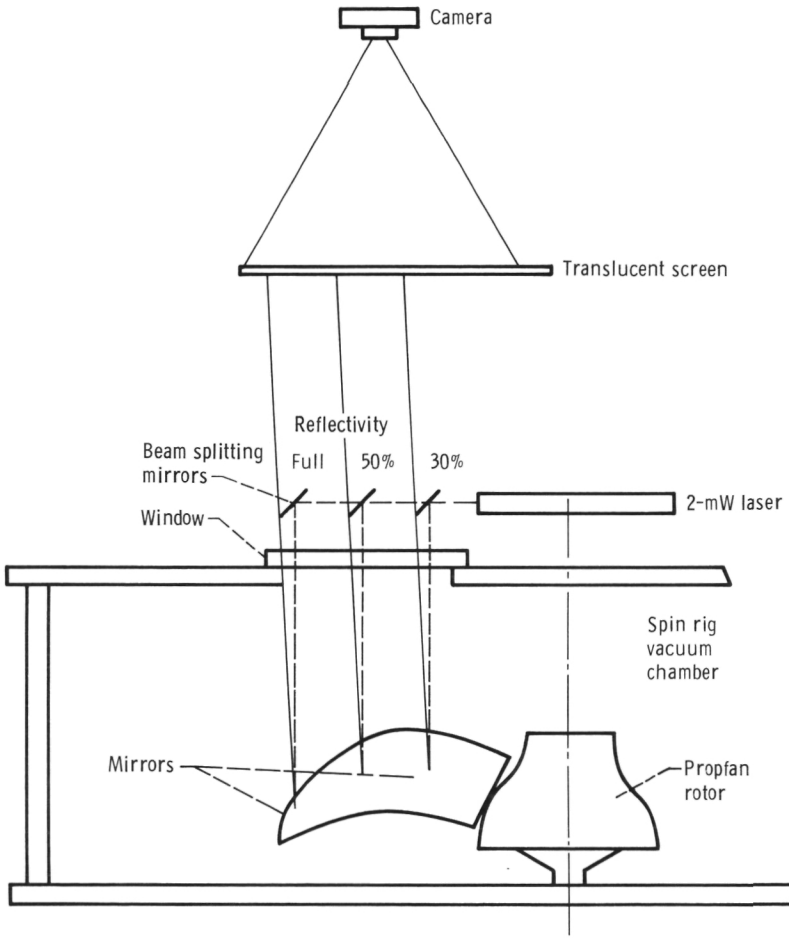

Laser mirror setup for measuring blade deflection

Two New Codes for Predicting Bladed-Disk Flutter

A modular code called ASTROP (Aeroelasticity and Structural Response of Propellers) and an aeroelasticity code incorporating three-dimensional aerodynamics have been developed. The ASTROP code, developed in-house, can predict flutter from structural data that are input in a modal form from any desired source. Extremely flexible, ASTROP can use any desired unsteady aerodynamics module; subsonic aerodynamics appropriate for advanced turboprop analysis is currently in use. The three-dimensional code, developed at Purdue University under a Lewis grant, has both steady and unsteady aerodynamic capability. It can be used to predict steady flow fields and airloads as well as the onset of flutter. The codes have recently been used together to predict flutter speed from the most thorough predictions yet made of the large steady-state deflections in highly flexible advanced turboprop blades.

These blades are now under study at Lewis and are being developed toward flight tests by industry under NASA contract. The very thin blades unbend and untwist, to a degree not experienced in fan, compressor, or turbine blading, because of a combination of centrifuged loads and air loads. An iterative solution of the mathematical equation governing the blade shape is required to obtain correct results because of strongly nonlinear geometrical effects. The three-dimensional code is used to estimate air loads on the basis of a first-approximation blade shape obtained from NASTRAN. The air loads are applied to obtain a better approximation of blade shape. After five or six iterations the resulting blade shape and vibration behavior are fed into ASTROP for flutter prediction. This is, to our knowledge, the most advanced flutter analysis method. □

Aileron Controls for Large Wind Turbines

Horizontal-axis wind turbines such as the DOE/NASA Mod-2 and others developed by industry during the past few years normally use relatively complex mechanisms to control blade pitch. In some designs the entire blade is rotated to change the pitch and thereby regulate rotor speed and power output. On the Mod-2 only the tip of the blade is rotated to accomplish the same purpose. This solution simplifies the design problem, but the tip support shaft is still forced to carry major structural loads.

Several years ago Lewis developed the idea of replacing blade pitch controls with aircraft aileron controls in an effort to provide a stronger and more economical rotor system. Aileron systems require smaller actuating devices, have proven their dependability in aircraft applications, and can be used with a continuous, one-piece blade structure.

Wichita State University, with the cooperation, support, and guidance

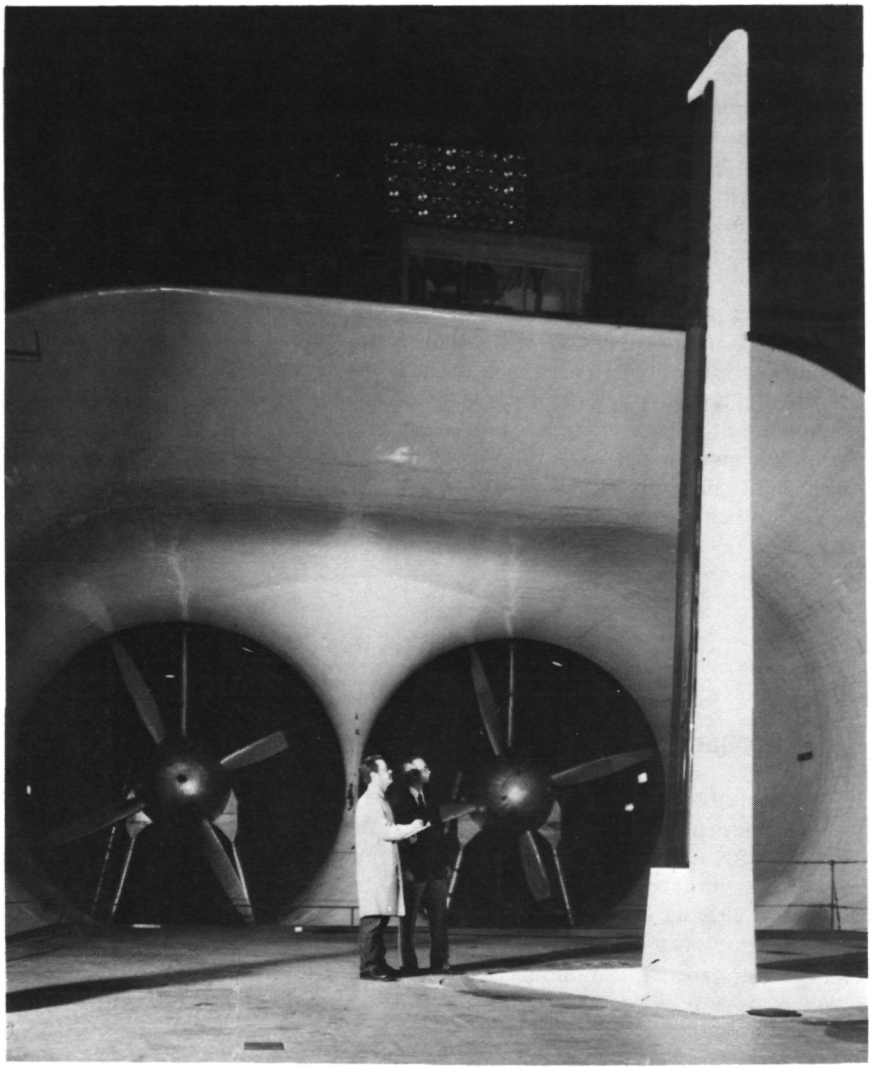

Advanced aileron control system in Langley wind tunnel

the Lewis wind energy engineers, developed and tested a variety of new and advanced aileron concepts in the WSU wind tunnel. The most promising configuration was found to be a trailing-edge flap, approximately 30 percent of the chord width of the blade wide and extending along the outer 30 percent of the blade span. A full-scale tip section, 24 ft long, with this aileron configuration, was tested in the Langley Research Center's 30- by 60-ft wind tunnel. The Langley tests provided the first direct measurements of lift and drag forces on a prototype wind turbine aileron and verified the design for further testing on a wind turbine rotor.

Field tests of the Mod-0 100-kW wind turbine with aileron control surfaces at the Lewis Plum Brook Station and wind tunnel tests have conclusively proven that aileron controls can provide the required degree of speed and power control for both normal and emergency operating conditions. The results of this test program are now being disseminated to the industry. The concept of aileron control systems has excellent potential for substantially lowering the costs and increasing the reliability of future wind turbines. □

General-Purpose Program for Brittle Material Design

Designing structural ceramics for heat engine applications requires new analysis techniques because of the intrinsic brittleness and statistical strength variations of ceramics. Advanced computational methods have been developed that rely extensively on finite-element solutions of required displacement, stress, and temperature fields, statistics of extreme values, and fracture mechanics. However, no comprehensive design code was available to engine manufacturers. In response to this need, Lewis developed the SCARE code.

The SCARE program uses MSC/NASTRAN analysis results and the Weibull weakest-link fracture strength distribution model. Polyaxial stress state response is calculated for volume-distributed flaws in macroscopically isotropic solids. Statistical material parameters can also be evaluated. Component fast fracture response, in terms of reliability and failure probability, is determined for any thermal or mechanical loading. Limited distribution to a number of ceramic component designers has been very encouraging, showing good agreement between measured and predicted structural response. □

IR–100
Servomechanism for Propeller Pitch Change

Advanced turboprop propulsion systems, now under development, offer the promise of substantial fuel savings for the next generation of commuter aircraft. Much more powerful and more accurate pitch-change mechanisms are needed to position these turboprop blades, some of which are 13 ft in diameter and carry 13 000 hp.

An innovative pitch-change mechanism, developed cooperatively by Lewis and the General Electric Company to meet these demanding requirements, was selected by Research & Development Magazine to receive a 1985 IR–100 award. This servomechanism uses fiber-optic controls; high-speed, advanced electric motor and generator technology; and a compact, traction-roller drive mechanism that amplifies motor torque 210 times. The system also features an onboard electric generator for pitch-change power generation. This eliminates the need for high-maintenance power sliprings or rotating hydraulic seals. Expected blade position accuracies, of the order of 1/20°, will minimize propeller noise and maximize fuel savings. Adaptations of this concept are suitable for a wide variety of heavy-duty, precision-pointing-mechanism applications such as missile aiming systems and large radar and antenna tracking drives. □

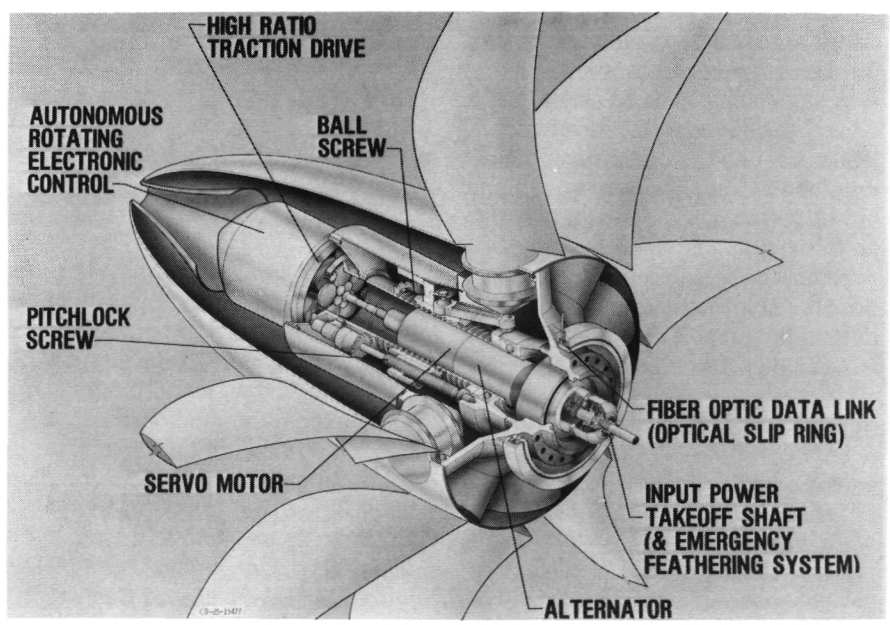

Autonomous, electromechanical pitch-change mechanism

Traction-Contact Torsional Stiffness Model

High-performance, fixed-ratio traction drives offer promise as positioning mechanisms. Applications include robotic hinge and pivot actuators, solar array and antenna drive positioners, and satellite control-moment-gyro gimbal drives. In such applications the drive's high ratio, low torque ripple, zero backlash, and high torsional stiffness are highly desirable. Zero backlash and high stiffness are required to produce a direct, continuous, "hard" link between output and input motion.

To perform a system response analysis of such a servomechanism, the tangential compliance of the contact must be estimated. Although closed-form solutions have been developed for the static case, no such solution was available for the transition from static to rolling. Thus a traction-contact torsional stiffness model was developed that solves for both static and rolling compliance by using linear elasticity theory for two elastic contacting bodies. Comparisons made to gear mesh stiffness show that comparably sized and loaded traction drive contacts are two to five times stiffer than gears. □

Three-Piece-Inner-Ring Roller Bearing

In conventional high-speed roller bearings with a one-piece inner ring, the roller lubrication holes and the undercut in the inner ring are sources of high stress concentration (photoelastic studies indicate a stress factor of about 10). At bearing speeds consistent with the next generation of aircraft turbine engines, the combined tensile stresses due to centrifugal and external loading can approach the tensile strength of the bearing material. Cracks, if formed at these holes, will quickly propagate through the brittle, through-hardened steels from which aircraft bearings are traditionally manufactured. The potentially explosive fracture that could result from this crack propagation is an unacceptable risk in the operation of future high-speed turbine engines.

These potential problems can be eliminated by employing a three-piece-inner-ring bearing configuration conceived at Lewis. A major advantage of this concept is the possibility of lubricating the inner ring without introducing any holes or slots in the load-carrying center ring, thus reducing the chance of fracturing the inner ring. With the three-piece-inner-ring bearing the possibility of fracture failure due to centrifugal stress can be further reduced by selecting higher-fracture-toughness (softer) steel for the side flanges that contain the feed holes. In addition, the three-piece inner rings can be lapped or honed to result in better surface finishes than those obtained by grinding as with a conventional one-piece flanged ring. Bearing tests at speeds 30 percent higher than that of current aircraft bearings have verified these anticipated benefits. □

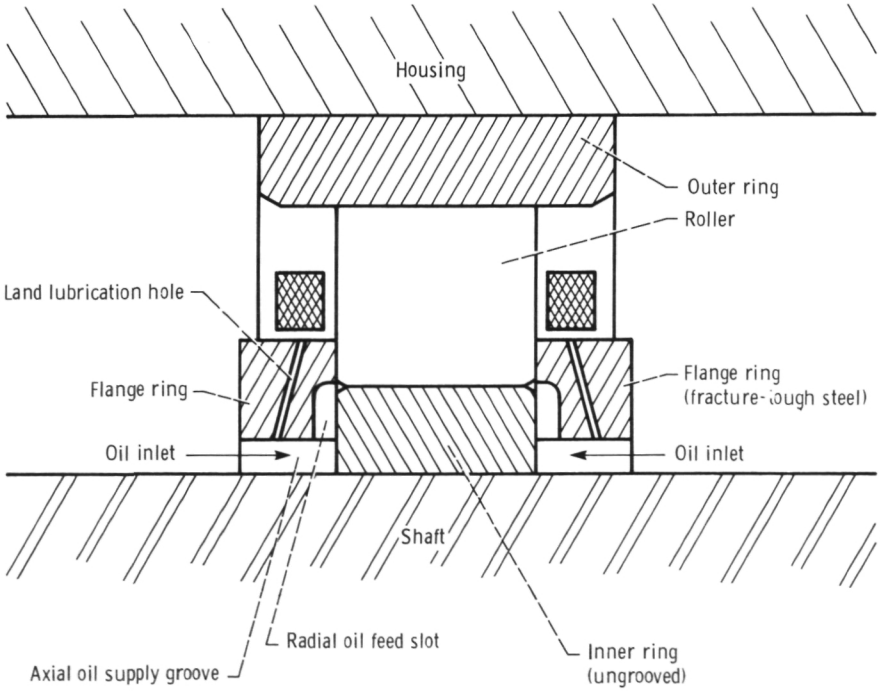

Three-piece-inner-ring roller bearing

Code for Determining Subsurface Stress in Rolling/Sliding Contacts

Machine elements such as rolling bearings, gears, cams, and traction drive transmissions are subject to failure from rolling-element contact fatigue. Such fatigue failures seriously restrict the operating life and reliability of machine components. Among the number of factors that contribute to fatigue failure, the effect of traction and slip on the state of stress between rolling elements is one that is not well understood.

A three-dimensional computer model has been developed by Battelle Columbus Laboratories, under contract to Lewis, for analyzing the state of stress beneath rolling/sliding contacts. The computer model determines the magnitude of reversing shear stresses beneath (and on) the surface of rolling/sliding contacts. Sliding in both the tangential and axial directions and line contacts as well as those due to a crowned roller are considered. The program makes it possible to examine the influence of traction on any one of the six subsurface stresses, but particularly on the maximum orthogonal reversing shear stress, thought to be responsible for fatigue failure. □

Spin Analysis of Machine Component Contacts

In the contact analysis of many machine components, such as bearings, gears, cams, and traction drives, the traction forces and resultant power losses due to sliding and rolling are of engineering importance. Spin, the result of a mismatch in contact radii on either side of the point of rolling, has a detrimental effect on traction contact performance. Spin occurs in concentrated contacts having conical or contoured rolling elements, such as those in traction drives or angular contact bearings, and is responsible for an increase in contact heating and power loss.

An algebraic method was developed to predict the spin velocities of arbitrarily shaped contacting bodies in rolling contact. A solution for the ideal, zero-spin-producing geometry was generated. It is now possible to minimize power loss and maximize fatigue life by suitably controlling the spin-producing contact geometry. The lubricant traction characteristics and special contact geometries that minimize spin can also be identified from this work. □

Three-Dimensional Computer Analysis Program to Interface Thermal and Structural Codes

A software package has been developed to transfer three-dimensional transient thermal information accurately, efficiently, and automatically from a heat transfer analysis code to a structural analysis code. The code is called 3–D TRANCITS (Three-Dimensional TRansfer ANalysis Code to Interface Thermal and Structural codes).

The 3–D TRANCITS code can handle different mesh densities for the heat transfer analysis and the structural analysis. It accurately and efficiently transfers the thermal information to produce nodal temperatures, elemental centroid temperatures, or elemental Gauss point temperatures for the stress model. Both finite-difference and finite-element heat transfer analysis codes can be coupled to both linear and nonlinear finite-element structural analysis codes.

For example, thermal output of both the MARC and SINDA heat transfer codes can be interfaced directly with 3–D TRANCITS, and it will automatically produce stress nodal point temperatures formatted for NASTRAN and MARC input. In addition to these codes, any thermal code can be interfaced with any structural code by using the neutral input and output forms supported by 3–D TRANCITS.

The architecture of the code is such that 3–D TRANCITS is both user friendly and easily modifiable. The code is constructed in modular form so that future modifications, or even different applications (e.g., pressure or boundary condition transfer) can be accomplished without a full rewrite. □

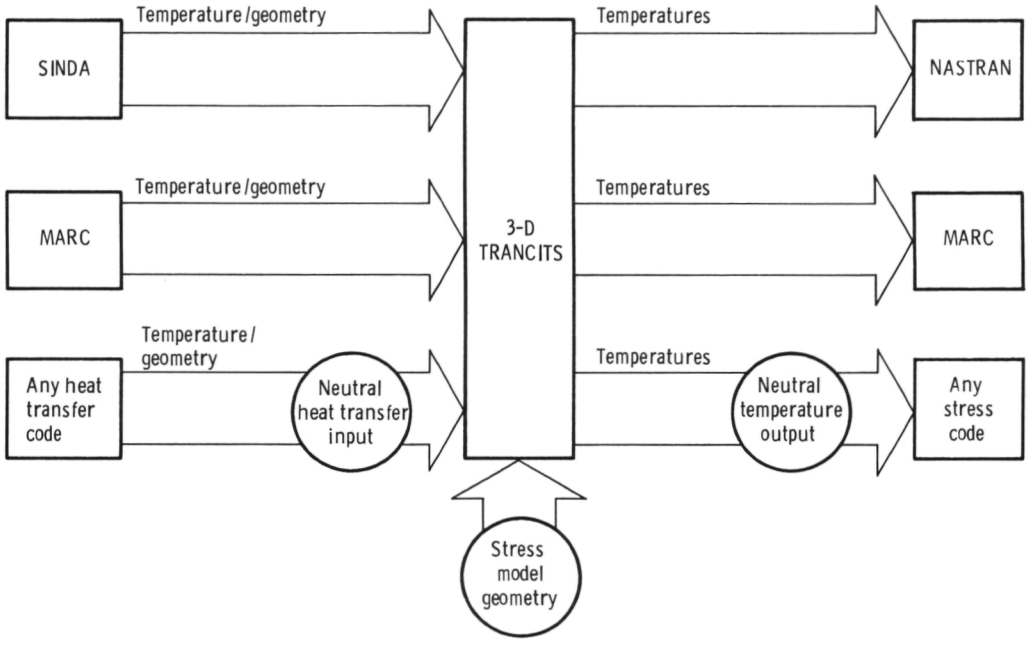

Overall program schematic for 3–D TRANCITS

Structural Durability of Fiber Composites

Predicting or even reasonably approximating the structural durability of fiber composite structures in service environments is a major concern in the fiber composite community. Fiber composite structures must resist mechanical loads (static, cyclic, and impact), variable temperatures, and moisture and combinations of these service environments (or hygrothermomechanical (HTM) conditions). The general procedure for designing fiber composites for HTM environments is to use empirical or other available data to select laminate configurations for the component. Tests are then conducted in the specified HTM environments, and the results are used to reconfigure the laminates, if necessary, to meet the design requirements. This procedure can be costly and time consuming and must be repeated for each new design.

This cumbersome procedure can be largely circumvented by a methodology that has been developed for predicting the structural durability and therefore service life of fiber

composites in HTM environments. The HTM effects on fiber composite stiffness and strength are predicted and then used to design fiber composite structural components for structural durability. This method has been used successfully to predict the structural durability of composite components designed for progressive fracture, high cycle fatigue combined with hot, wet conditions, and general laminates. □

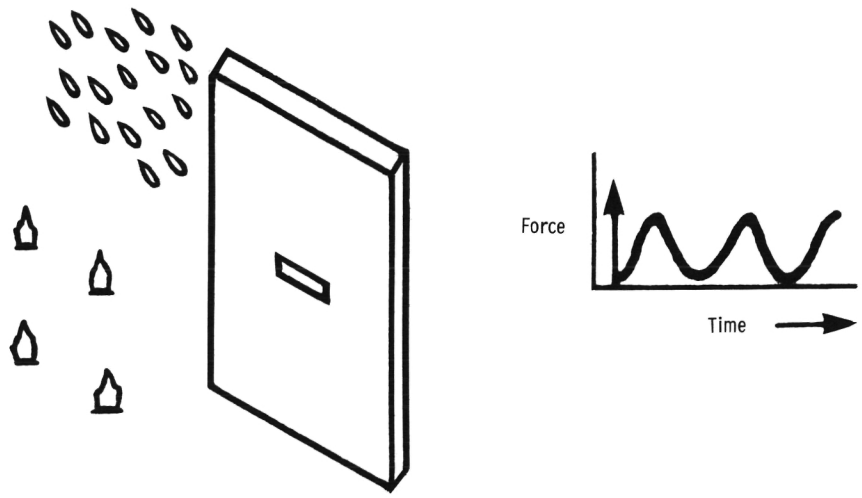

Environmental effects on defect growth in composite materials

Compression Failure Modes in Composites

In studies of the longitudinal compression behavior of unidirectional fiber composites, difficulties are frequently encountered with the proper interpretation of data containing considerable scatter. The scatter is associated primarily with the various failure modes that can occur with longitudinal compression fracture. The difficulties are compounded because compression testing is sensitive to factors such as Euler column buckling, specimen and fiber misalignment, and moisture.

Longitudinal compression behavior of unidirectional fiber composites is part of the composite micromechanics research being conducted at Lewis. A recent study used the IITRI test method to test both thick and thin specimens. Results showed that Euler column buckling was the predominant failure mode in the thin specimens and even in some of the thick specimens. There was also some evidence that end-tab debonding preceded specimen fracture, thus increasing the unsupported test section length and precipitating Euler column buckling.

To assess the end-tab debonding effects and the effects of any eccentricities (end attachment effects) on failure modes, a detailed finite-element analysis was performed of both the thick and thin specimens used in the experimental studies. The results show that eccentricities induce bending stresses that peak near the end tabs and cause flexural fracture. □

Ultrasonic Verification of Heat Treatment

Ultrasonic attenuation in metals and ceramics depends strongly on the material grain size. Recent efforts have attempted to relate ultrasonic scattering theory with material microstructure in order to determine the mean grain size. Success has been limited since the ultrasonic scattering theory is applicable to only a few nearly ideal metallic and ceramic microstructures. Lewis has developed alternative approaches to overcoming the problem of determining the material grain size from the ultrasonic measurement.

Ultrasonic attenation was measured for polycrystalline samples of nickel and copper with various grain-size distributions produced by heat treatment. Attenuation as a generalized function of frequency was determined for samples having known mean grain diameters. It was found that once this function was determined, it could be scaled to determine the mean grain size of other samples of the same material that were annealed to produce different mean grain diameters. The results suggest an ultrasonic, nondestructive approach for verifying grain size and heat treatment of metals. □

Improved Precision for Ultrasonic Measurements

Ultrasonic attenuation measurements are pivotal in the nondestructive assessment of material properties of critical aerospace structural components. An example is the use of ultrasound to verify the reliability of ceramics for high-temperature heat engines. This demands precise determination of attenuation properties of ceramic microstructures. It was discovered that even in dealing with ceramic specimens with relatively smooth "as ground" surfaces, considerable inaccuracies can occur in ultrasonic attenuation measurements. This is due to the heretofore unrecognized effect of surface microroughness.

Experimental evidence was developed showing the detrimental effects of this roughness over a broad frequency range. It was shown that these effects can be overcome and that precise attenuation measurements can be made only when the frequency dependence of the surface reflection coefficient is incorporated into the signal analysis processes. New methodologies and computer algorithms have been implemented on the basis of these findings. These are now being applied to ceramics in the as-ground condition, where the cost of polishing to remove microroughness would be prohibitive. □

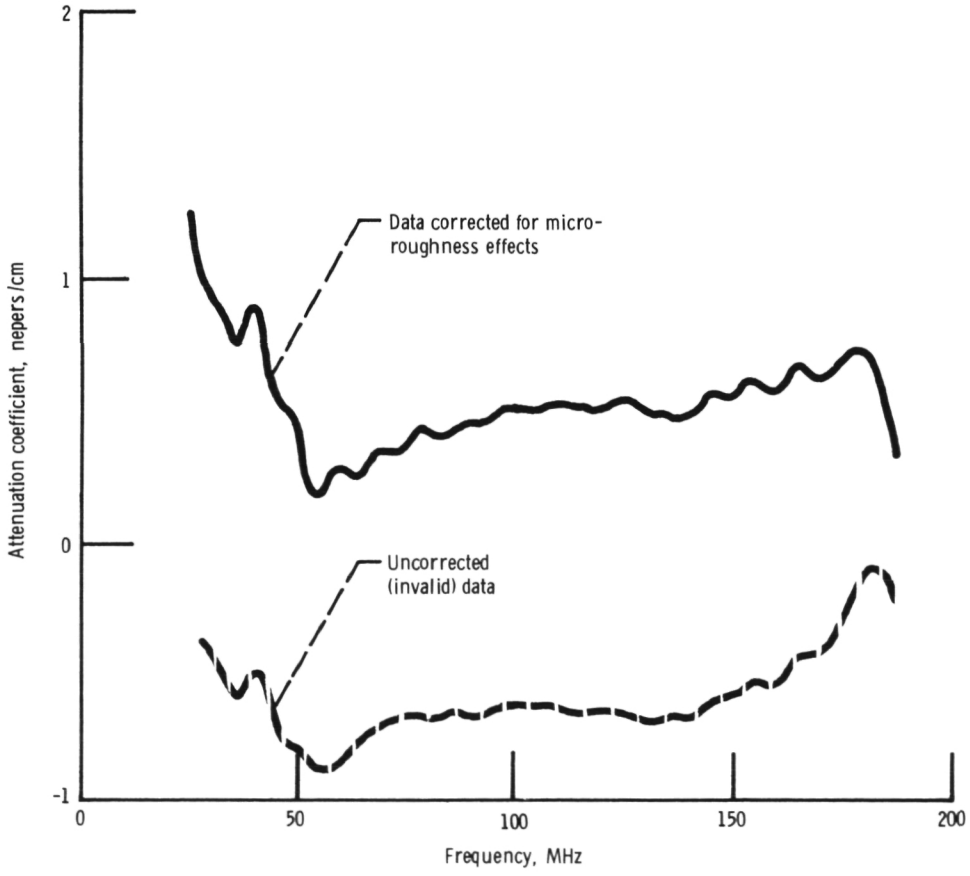

Data for Si_3N_4 ceramic modulus-of-rupture bar

Influence of Friction Dampers on Fan-Blade Flutter

Studies of supersonic torsional fan-blade flutter have typically simulated the aerodynamic instability by assuming a constant negative viscous damping. Consequently the results obtained did not provide a quantitative measure of the benefit of the dampers.

A study was conducted at Lewis to determine if the use of additional friction devices can allow the engine to operate at significantly higher fluid velocities while remaining stable. A lumped-parameter model with a single degree of freedom per blade was used to represent the blade disk. Two types of friction dampers, blade to blade and blade to ground, were considered.

For an advanced unshrouded fan stage with 28 blades, blade-to-ground dampers significantly increased the flutter Mach number from 1.2 to 1.6. Blade-to-blade dampers were less effective. □

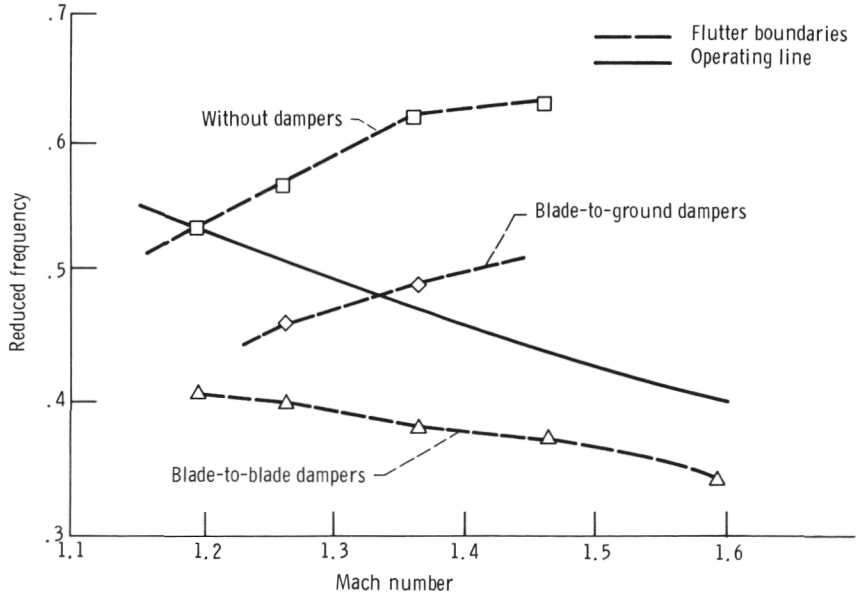

Flutter characteristics for various damper configurations

Rotor Vibration Control by Actively Controlled Bearings

Active control of the support properties of nonrotating bearing housings provides a new means for controlling rotordynamic unbalance and instability. A control method was demonstrated by simulation and experiment. The bearing housings are actuators for vibration control and are appropriately named "active control bearings."

Two methods for active bearing control were investigated. One is control by an optimal regulator with all state variable feedback, and the other is a quasi-modal control with velocity feedback based on a modal analysis. The rotor system was a two-degree-of-freedom system with one disk at the center of the span on flexible supports. The actuators were designed by using an electrodynamic transducer. The results obtained agreed with the simulations qualitatively. Therefore it is clear that unbalanced vibrations can be suppressed by active control bearings.

Because of the difficulty of estimating damping forces in practical rotating machinery, the optimal regulator method should prove to be superior to the quasi-modal method. The active control bearing system is effective not only for unbalanced forces but also for unstable forces or external forces transmitted from a foundation. □

Materials

Oxidation-Based Model for Thermal Barrier Coating Life

Thermal barrier coatings are finding use in gas turbine engines and other industrial applications where protection of a metal surface from a high-temperature environment is required. These coatings employ a thin layer of ceramic to insulate a cooler metallic component from the hot combustion gases in an engine. The expected life of the coating is of major importance to the engine designer.

A simplified model has been developed that predicts the expected life of a thermal coating subjected to a high-temperature environment. The model is based on the simplifying assumption that oxidation is the single important time-dependent factor that limits the life of these coatings.

Oxidation-induced strains combine with cyclic strains to induce slow-growth cracks in the ceramic layer. Ultimately this cracking leads to failure of the coating. An analytical expression is used to relate the weight gain of the coating due to oxidation and the thermal expansion mismatch strain to an effective strain. The growth rate of a crack per cycle is then related to this effective strain.

Failure occurs at a critical crack length that is related to the strain to failure. The final equation in the analytical model is a summation expression relating the number of cycles to failure to the strain and oxidation weight-gain parameters.

Life-cycle predictions by the model have been verified by comparison with specimens subjected to thermal cycles in a furnace. The agreement between prediction and experiment shows that the modeling approach has validity. However, more experimental work is required to delineate the effect of temperature level and other factors on the model parameters. Currently several engine companies are building on this model to produce engine-capable models that may be used by engine designers.

The paper that reported this work was written by Robert A. Miller and was selected as the Lewis Distinguished Paper for 1984–85. □

Strong and Tough Silicon Nitride Ceramic Composites

A method has been developed for processing silicon nitride ceramic composites that are stronger and tougher than monolithic silicon nitride materials processed under similar conditions. The method is based on reinforcing reaction-bonded silicon nitride (RBSN) matrices with high-modulus, high-strength, continuous-length silicon carbide (SiC) fibers produced by chemical vapor deposition. By infiltrating an aligned fiber array with silicon powder and then treating the green compact in a high-temperature nitriding atmosphere, SiC/RBSN ceramic composites have been formed with fiber volume fractions as high as 40 percent.

Under mechanical loading along the fiber direction, the high fiber modulus results in a matrix cracking stress greater than that for the ultimate fracture of an unreinforced matrix of equivalent density. Because of weak fiber-matrix interfacial bonding, matrix cracks propagate around the fibers and not through them. Thereby the strong fibers are left to carry the full composite load to higher strain levels. Thus fiber reinforcement avoids the brittle catastrophic failure typically observed in monolithic ceramics.

The improved toughness of this composite system coupled with ultimate strengths for fiber fracture that are measurably greater than those for the best commercial monolithic RBSN offers better prospects for the use of ceramic composites in high-temperature, structurally critical applications. □

Hot Corrosion of Ceramics

In a gas turbine, ingested sodium chloride can react with sulfur in the fuel to form molten sodium sulfate. This salt can then deposit on engine parts and lead to severe corrosion. To assess the effects of these deposits on candidate ceramic materials for gas turbines, silicon carbide bars were tested at 1000 °C in four atmospheres in a flame seeded with sodium chloride. Large amounts of sodium silicate formed, very likely by repeated oxidation and dissolution:

$$SiC + \frac{3}{2} O_2 \rightarrow SiO_2 + CO$$

$$SiO_2 + Na_2SO_4 \rightarrow Na_2SiO_3 + SO_3$$

This corrosion process resulted in dramatic pitting of the silicon carbide. Fractography studies indicated that these pits caused about a 30-percent strength decrease in the corroded material as compared with the as-received material.

Laboratory furnace experiments yielded similar results. The silicon carbide bars were coated with ~2.5 mg of sodium sulfate per square centimeter and placed in a laboratory furnace at 1000 °C. Specimens were examined at various intervals with both chemical analysis and microscopy. As in the burner case, oxidation and dissolution were the key processes. Furnace experiments also produced deep corrosion pits similar to those observed in the burner tests. These pits led to a substantial strength decrease below that of the as-received materials. The degree of strength degradation was related to the depth of the pit. Current experiments to elucidate the pitting mechanism may lead to eventual control of this corrosion problem. □

Compositional Effects in Single-Crystal Superalloys

The influence of composition on the high-temperature creep and tensile strength of single-crystal superalloys has been investigated. From the base-line alloy, Mar–M 247, a series of alloys was prepared with nickel as a substitute for the strategic metal cobalt and either nickel or tungsten as a substitute for the strategic metal tantalum. The highest creep-rupture lives were exhibited by alloys with no cobalt and high levels of tungsten. Fundamental relationships between creep-rupture properties and measured microstructural features were established. These results show that an alloy with a combination of improved properties and a low strategic element content is available and suggest further modifications to improve properties. □

Impact Resistance of Graphite/Polymer Composites

In response to the need to develop tougher, higher temperature resins for composite applications, basic studies were conducted to relate the low-velocity-impact resistance of graphite-fiber-reinforced composites with polymer matrix properties. Three crosslinked epoxy resins and a linear polysulfone were selected as composite matrices. As a group, these resins possess a significantly large range of mechanical properties that would allow subtle relationships between properties and impact toughness to be observed.

The mechanical properties of the resins and their respective composites were measured at room temperature. Undirectional and crossply composite specimens and neat resin specimens were impact tested with an instrumented drop-weight tester. Impact resistances of the specimens were assessed on the basis of loading capability, energy absorption, and extent of damage.

When the variables due to geometry and composition were taken into consideration, it was evident that there are relationships between polymer matrix properties and composite impact load and energy and the extent of impact damage. For example, internal damage became greater as the shear modulus of the composite material decreased. The amount of internal damage was determined by ultrasonic measurement. The effect of shear properties was more pronounced when the shear modulus was less than 600 ksi.

From the results of this study, matrix strength and modulus appear to be significant matrix properties that can influence composite impact resistance. □

Tungsten/Copper Composite for Improved Rocket Chambers

Some of today's rocket thrust chambers operate at chamber pressures of 3000 psia or above; this results in throat heat fluxes approaching 100 Btu/in.^{2} sec and wall temperatures to 1000 °F. To transmit this high heat load from the hot-gas-side wall to the coolant, while still providing sufficient strength to carry the pressure loads, high-strength copper-base alloys are used for the thrust chamber liner. The liner of the space shuttle main engine, for example, is fabricated from NARloy–Z, which contains 96 percent copper and has 93 percent of the thermal conductivity of oxygen-free, high-conductivity copper (OFHC).

However, the severe environment to which the thrust chamber wall is subjected irreversibly deforms and thins the cooling passage wall during each cycle of operation. Repeated thermal cycles cause cracks in the cooling passages walls and eventual failure of the thrust chamber. Therefore there has been a continuing effort to develop new materials to extend thrust chamber life.

A composite material made up of tungsten wire in a copper matrix offers the potential for extending thrust chamber life. The tungsten wire has the high strength necessary to carry the pressure loads and prevent deformation of the cooling passage wall; the copper has the high conductivity necessary to transmit the heat load to the coolant.

The fabrication consists of spraying a layer of liquid copper onto a steel mandrel that has the desired shape of the thrust chamber liner. Tungsten wire is then wrapped over the copper and a second layer of copper is applied in sufficient thickness to permit the machining of the cooling passages. Intermediate steps consist of hot isostatic pressings to densify the copper and to ensure intimate contact between the wire and the copper matrix. After the cooling passages have been machined, the mandrel is removed and the fabrication is completed conventionally. This process is applicable to both small and large thrust chambers.

Laboratory data show that the copper-tungsten composite has a rupture strength 80 percent higher than that of NARloy–Z with a thermal conductivity reduction of only 5 percent. Both cylindrical and contoured rocket thrust chamber liners were made with the copper-tungsten composite. □

Strengthening of Equiatomic Aluminides

Lewis is exploring the potential of equiatomic aluminides as structural materials for advanced aerospace applications such as hypersonic aircraft and space power systems. The intermetallic compounds FeAl and NiAl are lightweight, melt above 1500 and 1900 K, respectively, have good oxidation resistance, and can be alloyed to improve high-temperature strength.

FeAl and NiAl compounds have been alloyed with 1 to 5 at. % ternary additions of silicon (Si), titanium (Ti), zirconium (Zr), hafnium (Hf), chromium (Cr), nickel (Ni), cobalt (Co), niobium (Nb), tantalum (Ta), molybdenum (Mo), tungsten (W), and rhenium (Re). Third-element powders were blended with prealloyed binary powders of either FeAl or NiAl.

The alloys were consolidated into rods by hot extrusion at 1250 K for the FeAl and at 1350 K for the NiAl. Annealing studies on the extruded rods showed that for both the FeAl and NiAl the third-element addition at the 5 at. % level can be classified into three categories on the basis of the amount of homogenization and the extent of solid dissolution. Total solubility was exhibited by Fe, Cr, Mn, Co, and Ti (class I); partial solubility by Zr, Si, Hf, Nb, Ta, and Re (class II); and no apparent solubility by Mo and W (class III).

Constant-strain-rate compression tests were performed to determine the flow stress as a function of temperature and composition. The mechanical strength of FeAl and NiAl with third-element additions depended on the third element, its homogenization class, and the homogenization temperature. It appears that a new generation of materials for aerospace applications is feasible. Class II additions produced the greatest increase in strength over the binary aluminides. Transmission electron microscopy suggests that this increase in strength (3 to 5 times) is due to precipitation of fine ($\sim$200 nm), third-element-rich particles. □

Oxidation Effects on High-Heat-Flux Behavior of a Thermal Barrier Coating

The effect of oxidation on the high-heat-flux behavior of a thermal barrier coating has been evaluated by cyclically exposing preoxidized specimens to a 3000 °C nitrogen plasma. The thermal barrier coating consisted of a 0.025-cm-thick layer of air-plasma-sprayed ZrO_2–$7Y_2O_3$ and a 0.12-cm-thick layer of low-pressure-plasma-sprayed NiCoCrAlY applied over a 0.13-cm-diameter B1900 + Hf cylindrical substrate. A gradient of 800 °C was produced across the ceramic layer in each 0.5-sec exposure, much more severe than the gradient encountered on a gas turbine engine. Before exposure the specimens were preoxidized at 1200 °C for as long as 20 hours.

These coatings were tolerant to the high-heat-flux plasma flame for all but the most severe preoxidations. However, life degraded rapidly for preoxidation times in excess of about 15 hours at 1200 °C. The results indicate that at high heat flux, just as at low heat flux, oxidation is the most important time-at-temperature degradation mechanism for thermal barrier coatings. □

Temperature Dependence of $\gamma - \gamma'$ Lattice Mismatch in Nickel-Base Superalloys

The mismatch between the lattice parameters of the γ and γ' phases is one of several factors that can influence the mechanical properties of nickel-base superalloys. Controversy exists, however, over the exact role and importance of lattice mismatch in determining high-temperature properties. Thus Lewis made the first in-situ measurement of lattice mismatch at elevated temperatures. The results indicated that the predicted behavior of an alloy, based on room-temperature mismatch measurements only, can vary significantly from the actual behavior, determined by the measured elevated-temperature mismatch.

One example of the influence of lattice mismatch is the stress coarsening, or "rafting," observed in single-crystal superalloys. An alloy with positive mismatch at room temperature may have negative mismatch at high temperature, thus changing the orientation of the rafted structure. This work, was awarded the Materials Division 1985 "Order of the Enterprise" for its significant effect on material science and technology. □

High-Temperature Solid Lubricant for Foil Gas Bearings

A new self-lubricating coating of nickel-aluminide-bonded chromium carbide formulated with silver and group II fluorides (PS–200) was developed in a research program on high-temperature solid lubricants. One of its proposed applications is as a wide-temperature-spectrum solid lubricant for compliant foil gas bearings.

Friction and wear properties were obtained in a start/stop apparatus at temperatures from 25 to 650 °C. Uncoated, preoxidized Inconel X–750 foil bearings were operated against coated Inconel 718 journal surfaces. The foils were subjected to repeated start/stop cycles under a 14-kPa (2-psi) bearing unit loading. Sliding contact occurred during lift-off and coastdown at surface velocities less than 6 m/sec (3000 rpm). Testing continued until 9000 start/stop cycles were accumulated or until a rise in starting torque indicated the journal/bearing had failed.

Using the coating containing silver with the group II fluorides (PS–200) resulted in less than half the weight loss (wear) at 9000 cycles than the unmodified coating at failure (4500 cycles). □

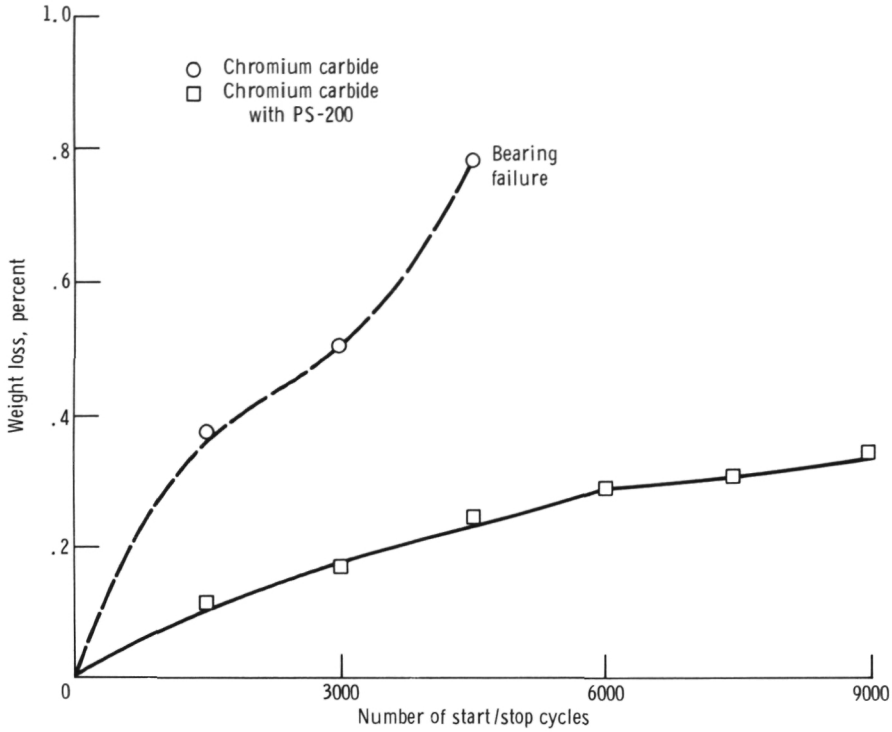

Lower wear with self-lubricating coating containing PS–200

Friction Behavior of Silicon and Gallium Arsenide

The sliding friction behavior of the semiconductors silicon and gallium arsenide in contact with pure metals was studied in order to improve bonding of conductors to semiconductors. Friction experiments were conducted at room conditions and in vacuum of 10^{-9} torr. Five transition metals (titanium, tantalum, nickel, palladium, and platinum) slid on a single-crystal silicon (111) surface in the [112] crystallographic direction. Four metals (indium, nickel, copper, and silver) slid on a single-crystal gallium arsenide (100) surface in the [011] direction. The sliding velocities were 1.4 mm/sec in room air and 0.2 mm/sec in vacuum. The loads were to 10 to 100 g in room air and 10 g in vacuum.

The friction depended on a Schottky barrier height φ_b formed at the metal-semiconductor interface. Metals with a higher barrier height gave lower friction. From titanium ($\varphi_b = 0.50$ eV) to platinum ($\varphi_b = 0.81$ eV) sliding on silicon, the coefficient of friction decreased linearly with increasing barrier height. The effect of the barrier height on friction behavior for chemically etched surfaces in vacuum was more specific than that for cleaved surfaces in room air. Similar effects were found for gallium arsenide, except that whereas silicon transferred to titanium, indium transferred to gallium arsenide. □

Thermal Oxidative Degradation of Unbranched Perfluoroalkylethers

Perfluoroalkylethers are a class of fluids that exhibit excellent thermal and oxidative stability. This characteristic combined with good viscosity, good elastohydrodynamic-film-forming capabilities, good boundary lubricating ability, and nonflammability makes these fluids promising candidates for high-temperature lubricant applications.

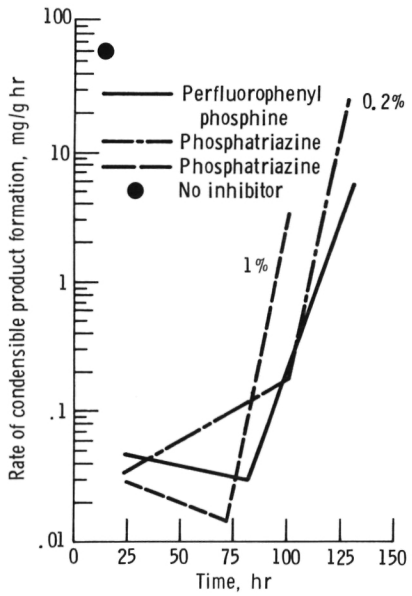

Effect of inhibitors on degradation of unbranched perfluoroalkylethers

Thermal oxidative degradation studies were performed on unbranched perfluoroalkylethers at 288 °C in oxygen. Metals and alloys studied included titanium, aluminum, and Ti–4Al–4Mn. The mechanism of degradation was by chain scission. Titanium and aluminum promoted less degradation than Ti–4Al–4Mn. Two inhibitors investigated (a perfluorophenyl phosphine and a phosphatriazine) reduced degradation rates by several orders of magnitude. Both inhibitors were effective for the same duration (75 to 100 hr). The phosphatriazine appeared to provide more surface protection. □

Ceramic Microstructure and Adhesion

Understanding ceramic microstructure and adhesion is a first step in Stirling engine design. When a ceramic is brought into contact with a ceramic, a polymer, or a metal, strong bond forces can develop between the materials. The bond forces will depend on the state of the surfaces, their cleanliness, and the fundamental properties of the two solids, both surface and bulk.

Ceramic surface properties that were correlated with adhesion included orientation, reconstruction, and diffusion as well as the chemistry of the surface species. Where a ceramic was in contact with a metal, their interactive chemistry and bond strength were considered. Bulk properties examined included elastic and plastic behavior in the surface regions, cohesive binding energies, crystal structures, and crystallographic orientation. Materials examined with respect to interfacial adhesive interactions included silicon carbide, nickel-zinc ferrite, manganese-zinc ferrite, and aluminum oxide. The surfaces of the contacting solids were studied both in the atomic, or molecularly clean, state and in the presence of selected surface contaminants.

Ceramic surface chemistry can change markedly with environment and temperature. Heating silicon carbide in a vacuum, for example, graphitizes the surface. The resulting graphite layer affects the adhesion and solid-state interactions of the silicon carbide with other surfaces. Depth profile analysis indicates the depth into the solid at which graphite exists. □

Adhesion Between Polymers and Evaporated Gold and Nickel Films

To obtain information on the adhesion between metal films and polymeric solids required for developing long-life space mechanisms, the adhesion force was measured by a tensile pull test. The adhesion strengths between polymeric solids and gold films evaporated on polymer substrates were about 1.11×10^6 N/m^2 on polytetrafluoroethylene (PTFE), about 5.49×10^6 N/m^2 on ultra-high-molecular-weight polyethylene (UHMWPE), and 6.54×10^6 N/m^2 on 6/6 nylon. The adhesion strengths for nickel films evaporated on these substrates were a factor of 1.7 higher than those for gold films on the same substrates.

To confirm quantitatively the effect of electron irradiation on the adhesion strength between a PTFE solid and metal films, the tensile pull test was performed on irradiated PTFE specimens. Nickel or gold was evaporated on PTFE surfaces irradiated with 2-keV electrons for various times. The improved adhesion for nickel was higher than that for gold. □

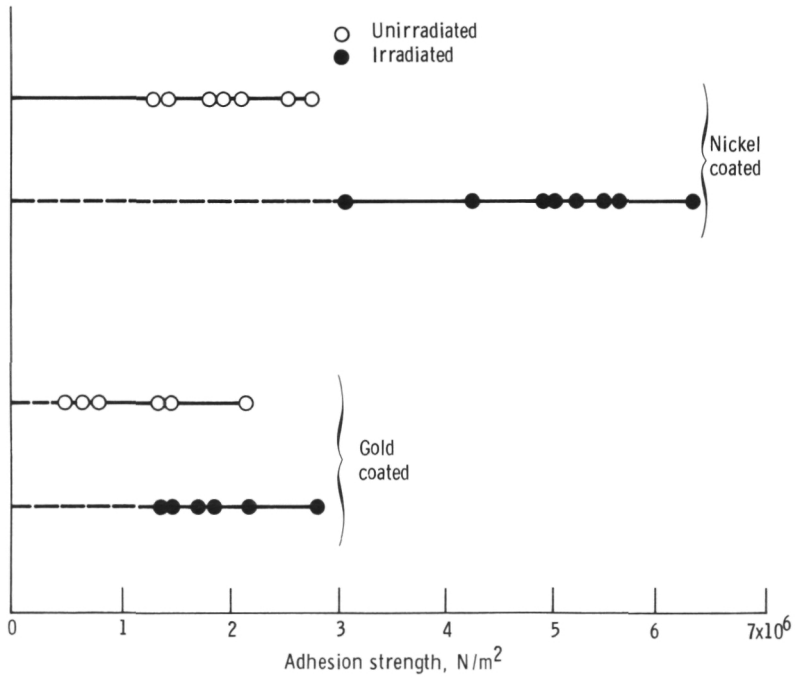

Adhesion strengths for PTFE surfaces

Title	Lewis contact	Telephone number, (216) 433-	Headquarters program office
Space Propulsion Technology:			
Centrifugal Pumps for Low-Thrust Rockets	Dean D. Scheer	2600	OAST
Turbine Loss Analysis	Louis A. Povinelli	5818	OAST
Altitude Capability at Rocket Engine Test Facility	Scott D. Meyer	2607	OAST
Compatibility of Grain-Stabilized Platinum with Resistojet Propellants	Margaret V. Whalen	2407	OAST
Rail Accelerators	Lynnette M. Zana	2409	OAST
High-Power Xenon Ion Thruster	Vincent K. Rawlin	2403	OAST
Low-Power, Direct-Current Arcjet	Francis M. Curran	2408	OAST
Tungsten-Reinforced Copper Thrust Chamber Liner	Richard J. Quentmeyer	2461	OAST
Composite Materials for Rocket Nozzles	Richard L. Dewitt	2601	OSF
Power Technology:			
Improved GaAs Concentrator Solar Cell	Henry B. Curtis	2231	OAST
Protective Coatings for Spacecraft Polymers	Michael J. Mirtich, Jr.	2225	OAST
Space Station Environmental Compatibility	Carolyn K. Purvis	3715	OSS
High-Power Linear Amplifier	Gene E. Schwarze	6117	OAST
Radiation Resistance of Power Switches	Gene E. Schwarze	6117	OAST
New Semiconductor Family	Gale R. Sundberg	6152	OAST
Analysis of Radiation-Cooled Transmission Lines	Gene E. Schwarze	6117	OAST
Simulation of Integrated Coal Gasifier/Fuel Cell Powerplants	Cheng-yi Lu	6137	OAST
Fuel Cell Electrode Modeling	Albert C. Antoine	6123	OAST
Free-Piston Stirling Engine for Space Power	Jack G. Slaby	6136	OAST
Second-Generation Automotive Stirling Engine	William K. Tabata	6139	OAST
Bipolar Nickel-Hydrogen Batteries	Robert L. Cataldo	5254	OAST
Advanced-Design Nickel-Hydrogen Cells	John J. Smithrick	5255	OAST
Structures:			
Vibratory Characteristics of Advanced Turboprops	Robert E. Kielb	6049	OAST
Two New Codes for Predicting Bladed-Disk Flutter	Krishna R. Kaza	6038	OAST
Aileron Controls for Large Wind Turbines	Darrell H. Baldwin	5522	OAST
General-Purpose Program for Brittle Material Design	John P. Gyekenyesi	3210	OAST
Servomechanism for Propeller Pitch Change	Stuart H. Loewenthal	3328	OAST
Traction-Contact Torsional Stiffness Model	Douglas A. Rohn	3325	OAST

Three-Piece-Inner-Ring Roller Bearing	Fredrick T. Schuller	3323	OAST
Code for Determining Subsurface Stress in Rolling/Sliding Contacts	Stuart H. Loewenthal	3328	OAST
Spin Analysis of Machine Component Contacts	Stuart H. Loewenthal	3328	OAST
Three-Dimensional Computer Analysis Program to Interface Thermal and Structural Codes	Robert L. Thompson	3321	OAST
Structural Durability of Fiber Composites	Christos C. Chamis	3252	OAST
Compression Failure Modes in Composites	Christos C. Chamis	3252	OAST
Ultrasonic Verification of Heat Treatment	Edward R. Generazio	6018	OAST
Improved Precision for Ultrasonic Measurements	Edward R. Generazio	6018	OAST
Influence of Friction Dampers on Fan-Blade Flutter	Robert E. Kielb	6049	OAST
Rotor Vibration Control by Actively Controlled Bearings	Kenzou Nonami David P. Fleming	6029 6013	OAST
Materials:			
Oxidation-Based Model for Thermal Barrier Coating Life	Robert A. Miller	5025	OAST
Strong and Tough Silicon Nitride Ceramic Composites	Ramakrishna Bhatt	5513	OAST
Hot Corrosion of Ceramics	Nathan S. Jacobson James J. Smialek	5498 5024	OAST
Compositional Effects in Single-Crystal Superalloys	Michael V. Nathal	3197	OAST
Impact Resistance of Graphite/Polymer Composites	Kenneth J. Bowles	3201	OAST
Tungsten/Copper Composite for Improved Rocket Chambers	Leonard J. Westfall	5526	OAST
Strengthening of Equiatomic Aluminides	Robert H. Titran	3200	OAST
Oxidation Effects on High-Heat-Flux Behavior of a Thermal Barrier Coating	Robert A. Miller	5025	OAST
Temperature Dependence of γ–γ' Lattice Mismatch in Nickel-Base Superalloys	Michael V. Nathal	3197	OAST
High-Temperature Solid Lubricant for Foil Gas Bearings	Harold E. Sliney	6055	OAST
Friction Behavior of Silicon and Gallium Arsenide	Donald H. Buckley	6061	OAST
Thermal Oxidative Degradation of Unbranched Perfluoroalkylethers	William R. Jones, Jr.	6053	OAST
Ceramic Microstructure and Adhesion	Donald H. Buckley	6061	OAST
Adhesion Between Polymers and Evaporated Gold and Nickel Films	Donald R. Wheeler	6074	OAST

Communications

IR–100
Baseband Processor

The expanding utilization of frequency and orbital slot resources puts ever greater pressure on designers of communications satellites to make the most efficient use of these resources. Studies indicate that a large community of user terminals can be most effectively served by time sharing the frequency-division channels at moderate to high burst rates. High-burst-rate operation also allows small user terminals to communicate directly with high-date-rate trunking terminals and thereby gain access to the terrestrial net. The key technology developments needed to make such a system feasible are rapid-acquisition, high-burst-rate demodulators, high-speed digital circuitry for routing individual messages, and coding and decoding circuitry to correct noise-induced errors on rain-degraded links.

A proof-of-concept (POC) model of the baseband processor has been built for Lewis by Motorola Government Electronics Group. The model demonstrates the burst demodulation of the uplink messages, the high-speed store-and-forward routing of the digital messages, and the subsequent remodulation of the messages prior to downlinking. It also demonstrates the capability to selectively decode and encode messages by using a forward error correction technique to mitigate a loss of signal due to rain fade.

The POC baseband processor has received a 1985 IR–100 award from Research & Development Magazine. A flight version of the baseband processor is being built as a part of the Advanced Communications Technology Satellite (ACTS) program. A 2- to 4-year flight demonstration program of the baseband processor is scheduled to begin with the launch of ACTS in 1989. □

30/20-GHz Ground Terminal Antennas

Two proof-of-concept ground terminal antennas have been successfully produced by Scientific-Atlanta for NASA's Advanced Communications Technology Satellite (ACTS) program: a 2.44-m-diameter nontracking antenna for experimental and low- to medium-data-rate applications, and a 4.72-m-diameter tracking antenna for high-data-rate and video applications. These antennas operate in the Ka band, transmitting at 27.5 to 30 GHz and receiving at 17.7 to 20 GHz. Both antennas have low side-lobe characteristics to accommodate close satellite spacing.

The 2.44-m-diameter antenna is manually adjusted for elevation and azimuth and is supported by an extremely rigid substructure to prevent deflection from wind loading. The 4.72-m-diameter antenna can provide complete telemetry, tracking, and command functions. The tracking techniques employ a unique Earth-reference optical system in conjunction with step tracking to maintain tracking accuracy. This system automatically compensates for deflections caused by wind loading, temperature differential, or satellite movement. □

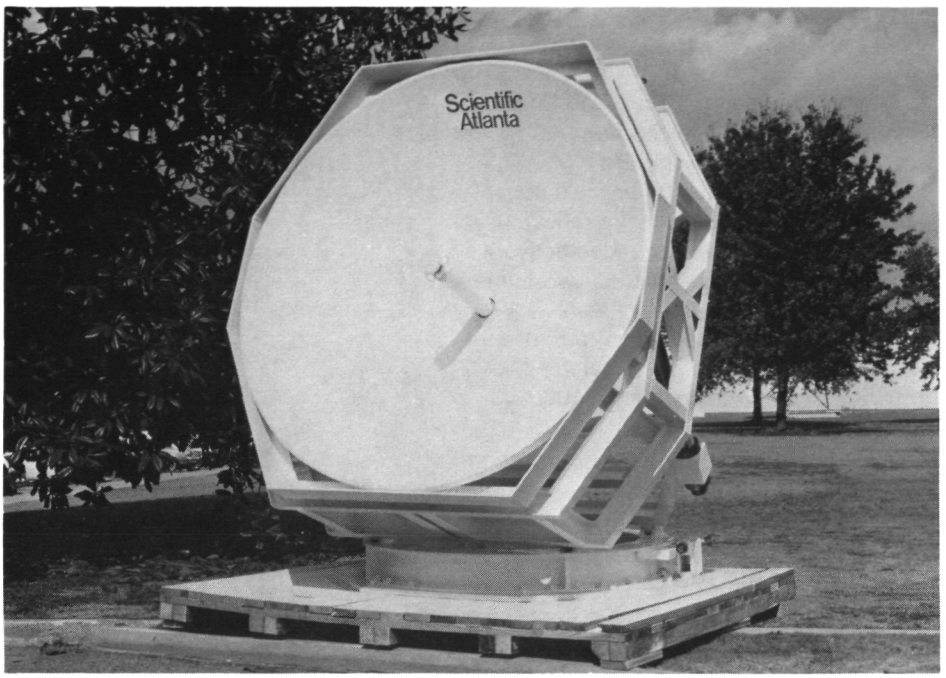

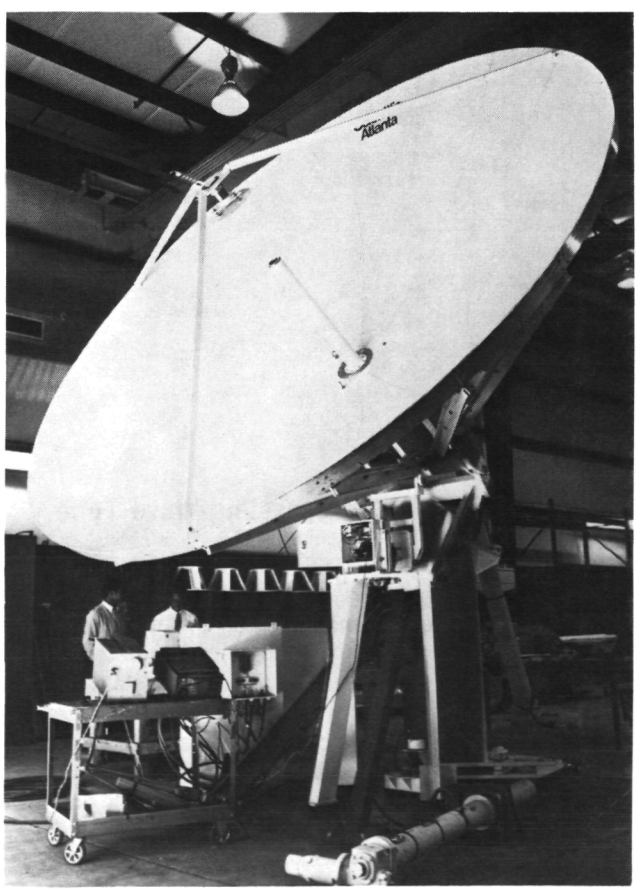

ACTS ground terminal antennas

IR-100
30/20-GHz Multiple-Beam Spacecraft Antenna

An advanced offset-fed spacecraft antenna system operating in the 30/20-GHz frequency bands has been developed for use on geosynchronous communications satellites. It can provide multiple radiating fixed-spot and regional-coverage scanning beams, alternative frequency bands for expansion of existing satellite services, and frequency reuse capability for conserving the frequency spectrum. Separate uplink and downlink antennas will transmit data in a time-division-multiple-access mode.

Each antenna will provide the narrow fixed-spot beams and communications coverage for high-volume traffic between major cities of the continental United States. Each beam will cover an area approximately 200 miles in diameter. The spacing of the spots across the country will allow reuse of the same frequency in many beams. The scanning beams will provide coverage for direct-to-user services to

remote areas according to the demands of the users.

Under parallel contracts to Lewis, TRW Electronic Systems Group and Ford Aerospace & Communications Corporation developed and tested proof-of-concept model antenna systems to demonstrate the technology. Both contractors used unique concepts in meeting the requirements for multiple beams, high gain, and optimum beam isolation. Contoured antenna reflector surfaces were developed to minimize radiofrequency losses, and feed-network arrays using multiple horns per beam, sharing of feed horn clusters, and high-speed ferrite switches, power dividers, and variable phase shifters were developed to switch the beams. This technology and its application to future communications satellites led to the multiple-beam antenna being selected as one of the top 100 developments in the nation in 1985 under the IR–100 awards program of Research & Development Magazine. □

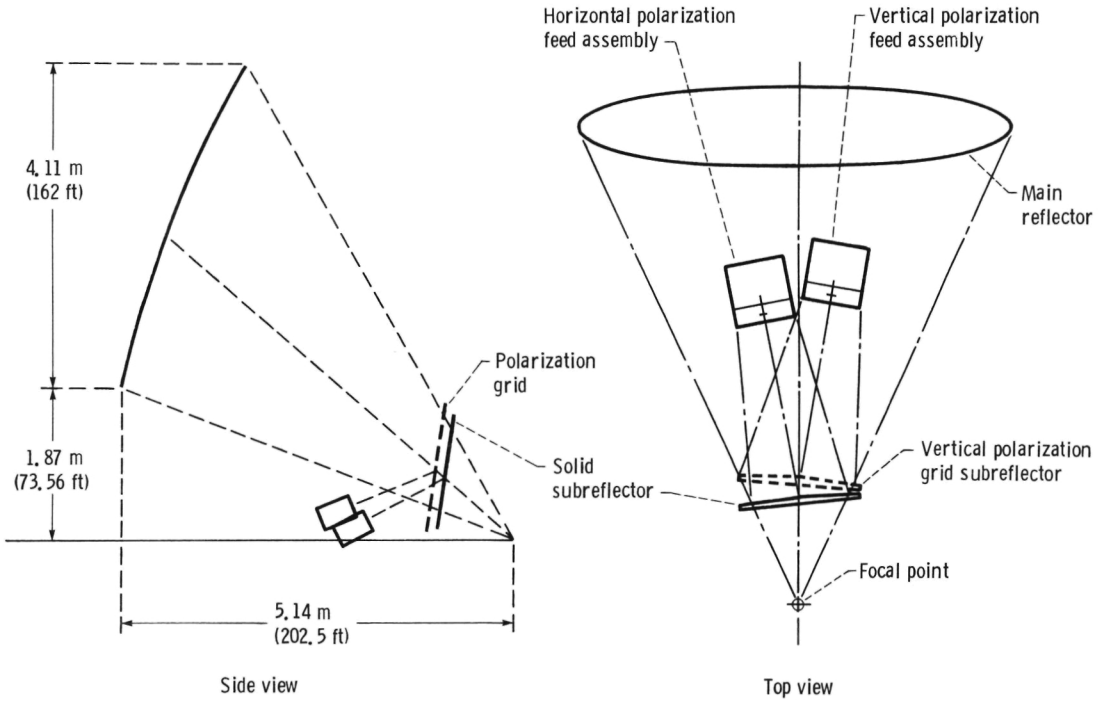

Offset dual subreflector for 30-GHz multiple-beam spacecraft antenna

60-GHz Traveling-Wave Tube

Future NASA and commerical satellite systems will require satellite-to-satellite communications links. An in-house study of this problem has determined that intersatellite links of relatively high frequency (61.5 GHz) are desirable because of the small antenna size and large available bandwidth. At this frequency with a linear power output of 25 W, the overall efficiency of a traveling-wave tube is of the order of 30 percent. At saturated power output it is 40 percent.

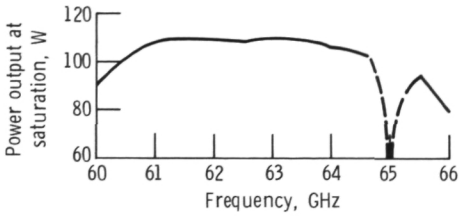

Power output at saturation as a function of frequency

The Hughes Aircraft Company received a 3-year contract on June 12, 1983, to develop a maximum of two coupled-cavity tubes to cover the range 59 to 64 GHz. The first tube developed was to have a single-stage depressed collector; the second, a four-stage collector. The first tube was built and tested with satisfying results. A saturated power output of 110 W was attained. Greater than 8-percent bandwidth was measured, allowing the full coverage of 59 to 64 GHz in one tube. Overall efficiency of 36 percent was achieved with a single-stage depressed collector.

A second tube with a multistage depressed collector is now being built. On the basis of the single-stage results, the goal of over 40 percent efficiency should be achieved. □

IR-100
20-GHz Transmit Module

Advanced phased-array antenna systems have been identified as a major factor in achieving minimum cost and efficient use of the frequency and orbital resources for future generations of communications satellite systems. Using solid-state monolithic microwave integrated circuits (MMIC) as the radiofrequency source offers weight, cost, and efficiency advantages over conventional rf sources. A single MMIC module can perform many electronic functions, thus providing consistent performance. The MMIC module does not require external tuning. Other problems, such as parasitics and device value uncertainties, normally associated with nonmonolithic components are minimized.

Lewis is pursuing MMIC developments that promise to have a maximum effect on future communications systems in the 30/20-GHz frequency range. Rockwell International under contract to Lewis has developed a 20-GHz MMIC transmit module with amplification and phase shift capabilities. The module's 5-bit phase shifter provides 32-step phase shift control from 0° to 360° with 16-dB gain and 200-mW output power. This module development was judged to be one of the significant new technologies of 1985 and was awarded a prestigious IR-100 award by Research & Development Magazine. □

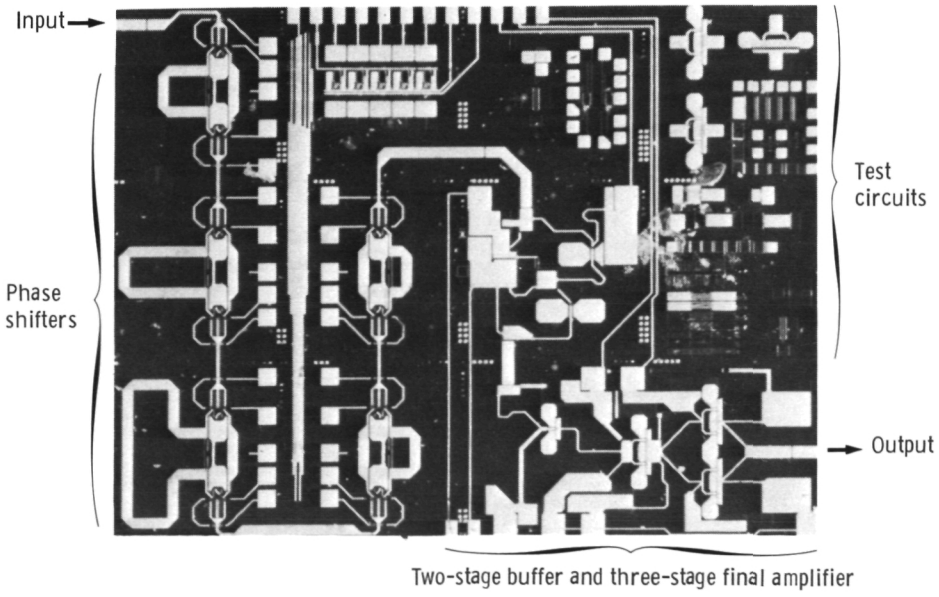

20-GHz monolithic transmit module

Monolithic 30-GHz Phase Shifter

Under contract to Lewis the Honeywell Physical Science Center is developing 30-GHz monolithic receive modules and submodules for experimental evaluation. The receive module comprises four submodules: a low-noise amplifier, a phase shifter, a gain control, and a mixer submodule. The phase shifter submodule is the first monolithic phase shifter to be made at frequencies above 20 GHz.

One-hundred phase shifter submodules have been delivered for experimental evaluation. A switched-transmission-line phase shifter using unbiased field-effect transistors was used to achieve the 45°, 90°, and 180° bits, and a loaded-line phase shifter was used to achieve the 11.25° and 22.5° bits. The 5-bit (32 state) phase shifter operates from 27.5 to 30.0 GHz. □

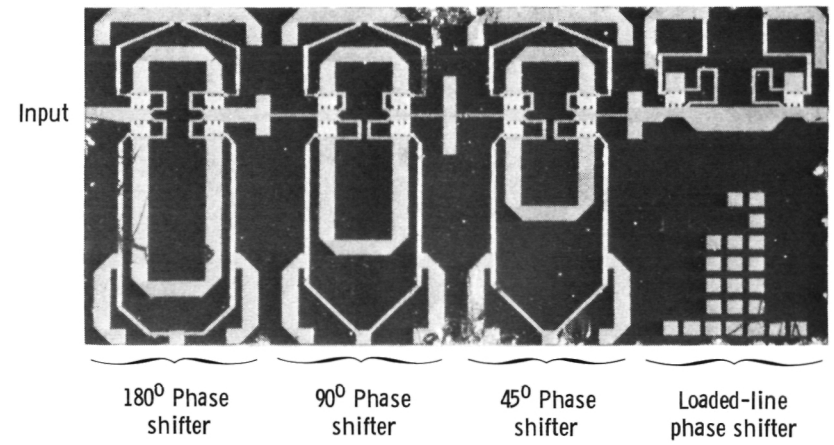

30-GHz monolithic phase shifter

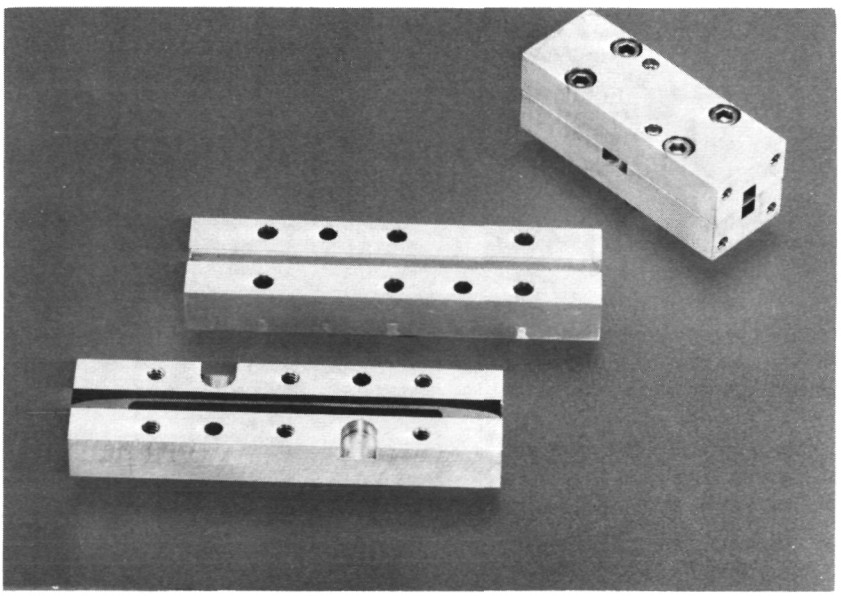

26.5- to 40-GHz waveguide-to-microstrip transition in test fixture

Waveguide-to-Microstrip Transitions

The use of frequencies above 18 GHz for both government and commerical communications programs is expected to increase rapidly. Systems using these higher frequencies will probably incorporate gallium arsenide microwave monolithic integrated circuits (MMIC) to exploit their inherent advantages in cost, weight, and efficiency. State-of-the-art MMIC technology uses the microstrip transmission line for circuit inputs and outputs, but in communications system configurations the use of the waveguide is appropriate. Therefore a means had to be developed of coupling microstrip circuits to waveguide systems while maintaining the inherent advantages of the MMIC.

Lewis developed the design procedure for a microwave microstrip-to-waveguide transition that is inexpensive to fabricate. The wide bandwidth and low loss characteristics of the transition are ideally suitable for communications systems where MMIC's are used. □

30/20-GHz Communications System Test Bed

The extension of commerical communications services into the 30/20-GHz frequency bands has necessitated the development of numerous new technologies at these frequencies. In particular over the last 5 years, NASA has sponsored the design of receivers, switches, solid-state transmitters, and traveling-wave-tube transmitters at 30 and 20 GHz.

An evaluation of the performance of these components in transmission of high-rate (220 megabits/sec) digital data is important as guidance both in further development and in applications such as NASA's Advanced Communications Technology Satellite (ACTS).

The test bed, which is now operational, provides for generation of pseudorandom data at 200 megabits/sec, serial-minimum,shift-keyed modulation, calibrated noise insertion, upconversion to 30 GHz, translation to 20 GHz, downconversion to 3.3 GHz, demodulation, and error checking. Components may be inserted at any point in the system and bit-error-rate data generated.

The system was first applied to a 30-GHz, 200-W traveling-wave tube proposed as the ground terminal amplifier for the ACTS high-rate stations. Results indicate that the proposed tube would introduce degradations of approximately 2 dB. □

Title	Lewis contact	Telephone number, (216) 433–	Headquarters program office
Baseband Processor	Scott M. Klement	3535	OSSA
30/20-GHz Ground Terminal Antennas	Ronald J. Schertler	3566	OSSA
30/20-GHz Multiple-Beam Spacecraft Antenna	Royce W. Myhre	3541	OSSA
60-GHz Traveling-Wave Tube	Francis E. Kavanagh	3509	OAST
20-GHz Transmit Module	Godfrey Anzic	3570	OAST
Monolithic 30-GHz Phase Shifter	Godfrey Anzic	3570	OAST
Waveguide-to-Microstrip Transitions	Godfrey Anzic	3570	OAST
30/20-GHz Communications System Test Bed	Regis F. Leonard	3499	OSSA

Space Station Systems

IR-100
Multihundred-Kilowatt Roll Ring Assembly

The multihundred-kilowatt roll ring assembly for space power transfer across a rotary joint is being evaluated by Lewis in support of the space station program. The potential advantages of the roll ring for space applications include high efficiency, large power transfer (ac or dc), elimination of sliding friction, low turning torque, and long life.

The roll ring transfers power across a rotating joint through flexures that rotate between the conducting rings. Ten flexures per ring provide redundant current paths. The flexures are slightly compressed for positive contact with both conducting rings.

The roll ring assembly can transfer 400 kW of power (four circuits; 500 V dc and 200 A per circuit). The roll ring assembly has been tested with currents from 100 to 200 A for 300 000 revolutions, which represents more than 60 years of use on the space station. The roll ring assembly has also completed 3 months of high-voltage (500 V dc) testing. The power capability of this assembly, 400 kW, can satisfy the space station rotary joint need of 150 kW with margin. Power is transferred with 99.985-percent efficiency.

The roll ring assembly was developed and fabricated for Lewis by Sperry Flight Systems of Phoenix, Arizona. □

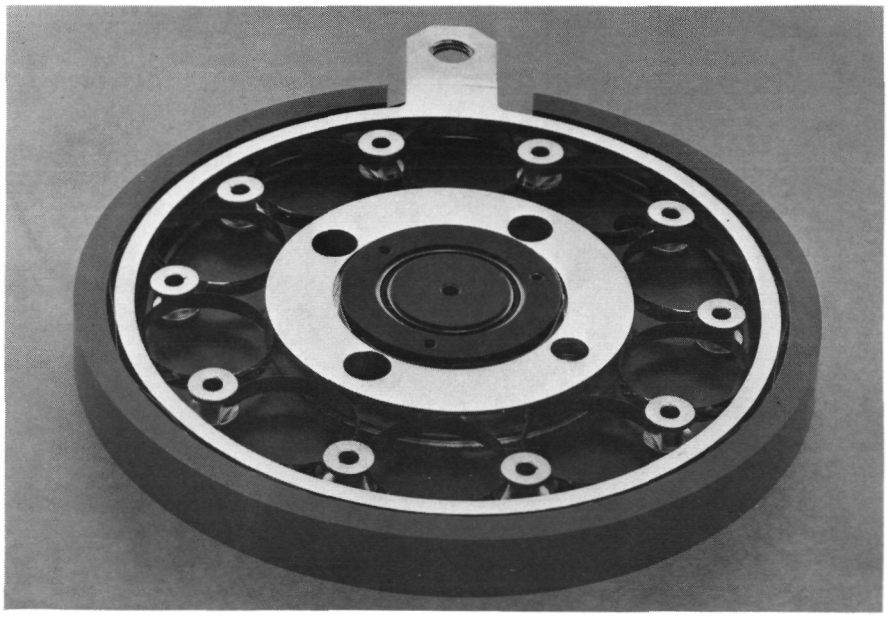

Roll ring assembly

Alkaline Water Electrolysis Technology

Endurance testing of alkaline electrolyzer components has shown that the technology is sufficiently advanced to be considered for the energy storage subsystem of the space station. When coupled with a fuel cell, an electrolyzer forms half of a regenerative fuel cell system. This system would be used on the space station, in conjunction with a solar cell power generation system, to store energy in the form of the common reactants hydrogen, oxygen, and water.

The electrolyzer would function by consuming electric power during the daylight portion of an orbit to decompose water into hydrogen and oxygen. The fuel cell would subsequently recombine this hydrogen and oxygen into water to produce power during the eclipse portion of an orbit.

Life Systems, Inc. (LSI), has been developing advanced alkaline water electrolysis technology since 1979, under contract to Lewis. Acid

electrolyzers had been well developed for life-support systems, but an alkaline electrolyzer was desired because it would be easier to integrate with the space power alkaline fuel cell.

Work at LSI has been concentrated in two major areas, the first of which is development of lightweight, long-life, high-performance cell components. Cell components under development include electrodes, separators, and cell frames. Endurance testing of these components in single cells has recently passed 40 000 hours. In the mechanical ancillary component area, work has been directed toward development of coolant control assemblies, fluids control assemblies, and fluids pressure controllers. These components have accumulated over 20 000 hours of endurance testing. Endurance testing has progressed to the subsystem level. □

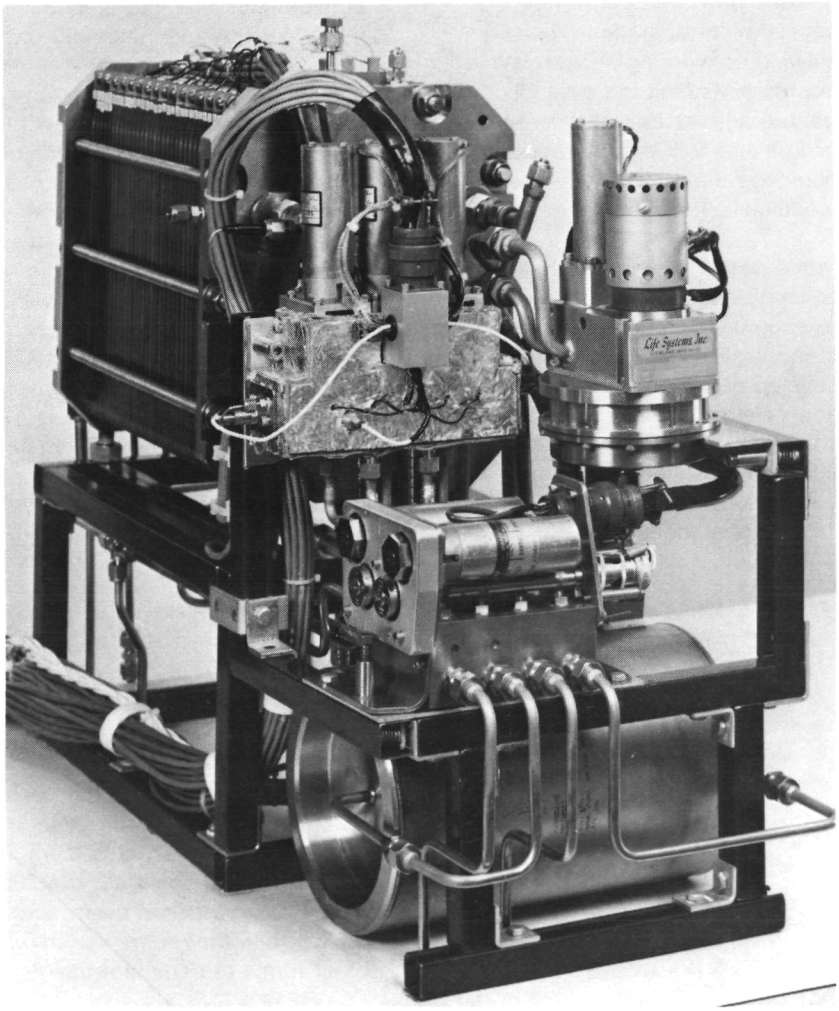

Alkaline electrolyzer

Title	Lewis contact	Telephone number, (216) 433–	Headquarters program office
Multihundred-Kilowatt Roll Ring Assembly	Fred Teren	5310	OSS
Alkaline Water Electrolysis Technology	Dean W. Sheibley	5378	OSS

Computational Technology Support

Acceleration of Convergence

The practical solution to many problems that arise in research at Lewis may ultimately require the summation of a slowly converging (or even diverging) infinite series or the computation of the limit of a sequence of vectors. Without using any special device, approaching the desired limit in slow convergence may become very costly; in divergence a limit cannot be reached at all.

It is the purpose of convergence acceleration methods to make a slowing converging sequence approach its limit more rapidly (i.e., get the answer from just a few terms) or to make a divergent sequence converge to a quantity that has meaning to the scientist or engineer.

In the past 8 years there has been a concentrated effort at Lewis to study existing acceleration methods both theoretically and numerically, to develop new techniques, and to find new or more efficient algorithms for implementing existing techniques. This effort has resulted in a number of publications and presentations at international meetings.

Early in the program an extensive theoretical and numerical study of acceleration methods led to the development of a robust and adaptive general-purpose algorithm called HURRY, now installed on the IBM 3033. This routine can accelerate a great many slowly converging sequences and predict the accuracy of its result with astonishing precision.

The idea of accelerating the convergence of vector sequences is important for fluid mechanics or structures problems, many of which involve iterative processes. One difficulty with this approach is that the "vectors" may have hundreds of thousands of components, so that computer memory and storage requirements become excessive. Recently a new technique was developed at Lewis to cope with this problem. The new low-memory technique has vastly improved accuracy over standard iterative approaches. Although it takes a little longer to start accelerating than current methods, is well worth it if memory is a constraint. □

GRAPH3D Computer Graphics

Computer graphics has long been recognized as a primary method for informatively representing computer data. At Lewis, computer graphics usage has increased even more rapidly than the enormous increase in other forms of computer usage.

The advent of the Cray-1S and new mainline computers has enabled the operation of large applications programs and has also offered a resource to other sectors of Lewis besides science and engineering. The net effect is the production of such large amounts of data that the only sensible means of information extraction is through graphics and thus an increased diversity in the requirements for computer graphics.

To meet these demands, a previously developed scientific graphics system known as GRAPH2D has been completely restructured. The new system, appropriately named GRAPH3D, is in accord with SIGGRAPH core graphics standards and is the most powerful and unique scientific graphics system available in the nation today.

GRAPH3D features a full three-dimensional viewing environment, full output device independence, full transparency to existing two-dimensional-based applications, hidden line and surface capabilities, full color, structures for full raster support, and powerful character-handling facilities. Over 175 new graphics modules representing approximately 70 000 lines of code were generated in this effort, resulting in a total system of approximately 300 modules and 100 000 lines of code.

GRAPH3D brings with it addition of the z-axis and color as a nearly continuous variable, thereby greatly enhancing the representation of engineering and scientific data. Features such as report-quality character fonts, perspective, and color-raster internals allow new applications in the management and administrative sector of Lewis.

In addition to the software development seven kinds of graphics output devices exceeding $1 million in total value have been acquired over the last fiscal year for use with the Lewis centralized computing network.

GRAPH3D support for these devices is now or will be shortly available. When this support is fully in place, Lewis will have effectively doubled the number of end-user remote accesses and added the functions of color, raster, and local three-dimension and will have increased its per-page graphics production capacity by orders of magnitude. □

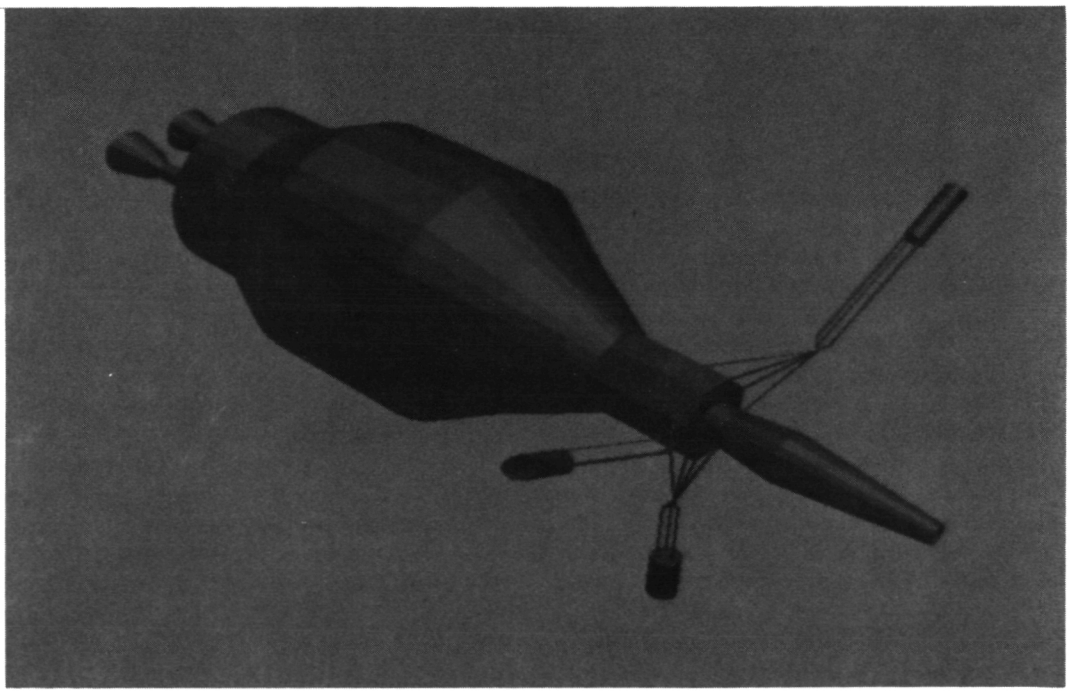

Example of GRAPH3D computer graphics

Title	Lewis contact	Telephone number, (216) 433–	Headquarters program office
Acceleration of Convergence	William F. Ford	5171	OAST
GRAPH3D Computer Graphics	William F. Ford	5171	OAST